`

UNIVERSITY OF CALIFORNIA SAN DIEGO

Real time cell proliferation and live cell cycle tracking analyses reveal dynamic changes and inhibitory responses to therapeutic drugs for treating prostate cancer.

A thesis submitted in partial satisfaction of the requirements
for the degree Master of Science

in

Biology

by

Evodie Koutouan

Committee in charge:

Professor Christina Jamieson, Chair
Professor Douglass Forbes, Co-Chair
Professor Julian Schroeder

2022

The Thesis of Evodie Koutouan is approved, and it is acceptable in quality and form for publication on microfilm and electronically.

University of California San Diego

2022

DEDICATION

I dedicate this work to my family, my lab, my friends and loved ones who believed in me and supported through this accomplishment.

EPIGRAPH

Trust in the Lord with all your heart; do not depend on your own understanding.

Proverbs 3:5

TABLE OF CONTENTS

LIST OF FIGURES

LIST OF ABBREVIATIONS

CLIC1	Chloride intracellular channel protein 1
CRPC	Castration Resistant Prostate Cancer
PC3	Human prostate cancer cell line
PCa	Prostate Cancer
ROR1	Receptor tyrosine kinase-like orphan receptor 1
FUCCI	

ACKNOWLEDGEMENTS

Chapter 1, 2, and 3 includes work in preparation for submission for publication Jamillah Murtadha, **Evodie Koutouan**, Chris Oh, Michelle Muldong, Niloofar Etemadfard, Hae Soo Choo, Navyaa Sinha, Sanghee Lee, Christina Wu, Catriona Jamieson, Christopher Kane, Terry Gaasterland, Rana Mckay, Nicholas Cacalano, Anna Kulidjian, Charles Prussak, and Christina Jamieson.

The thesis author was the second author of this paper.

ABSTRACT OF THE THESIS

Real time cell proliferation and live cell cycle tracking analyses
reveal dynamic changes and inhibitory responses to
therapeutic drugs for treating prostate cancer.

by

Evodie Koutouan

Master of Science in Biology

University of California San Diego, 2022

Professor Christina Jamieson, Chair
Professor Douglass Forbes, Co-Chair

Prostate cancer remains the second leading cause of cancer death among men over 50 years old in the United States. Docetaxel is a taxane drug currently being used as a chemotherapy for advanced prostate cancer. However, prostate cancer patients often develop resistance to chemotherapy drugs. Therefore, we are interested in investigating new pathways that have the potential to overcome this resistance. From preliminary, independent analyses of ours and others, two new pathways have been shown to be important in advanced, therapy-resistant prostate cancer: ROR1 and CLIC1. ROR1 is the Receptor tyrosine kinase-like orphan receptor 1, an

onco-embryonic antigen, which binds the WNT5A ligand and mediates non-canonical WNT signaling. The Chloride intracellular channel protein 1 (CLIC1) is known to be an important biomarker in several cancer types including prostate cancer. We sought to investigate the potential synergy of inhibitory therapies targeting ROR1 and CLIC1 with docetaxel.

We hypothesized ROR1 and CLIC1 pathways as potential targets for therapies that can work either alone or in synergy with Docetaxel to inhibit prostate cancer progression. In this study, we sought to investigate the effect on cell proliferation and cell cycle of Docetaxel treatment and the inhibition of ROR1 and CLIC1 pathways.

Through the optimization of cell-based assays using the Incucyte live cell microscope imaging technology, Docetaxel's inhibitory effects on cell proliferation via G2 arrest was confirmed. Strikingly, our results revealed that without ROR1 expression, Docetaxel treatment leads to increased inhibition of cell proliferation, which we predict could lead to better outcomes in the clinic.

INTRODUCTION

Prostate cancer remains one of the top leading causes of cancer death among men over in the United States (*SEER*, 2021). Current treatments against prostate cancer involve the targeting of androgen receptor (AR) signaling (Fizazi et al., 2012; Dhingra et al., 2013). However, despite the therapies being used, a significant number of patients develop a more severe form of the disease diagnosed as metastatic castration-resistant prostate cancer (CRPC) (Crona & Whang, 2017; Gillessen et al., 2020; Vlachostergios et al., 2017), with a considerable high death rate (*SEER*, 2021).

A chemotherapy drug used for treating CRPC is the taxane, docetaxel, which acts as an inhibitor of microtubules' depolymerization through binding of β-subunit of α/β-tubulin dimers (Perez 2009). This action leads to the impairment of microtubules dynamics necessary for mitosis, causing a cell cycle arrest (Jordan & Wilson, 2004; Jordan 2002).

Unfortunately, CRPC still remains lethal (Kirby et al., 2011; Grasso et al., 2012). Thus, there is an urgent need to develop new treatments and therapies as well as new combinations with current standard of care therapies against prostate cancer progression and its ability to metastasize.

ROR1

Receptor tyrosine kinase-like orphan receptor 1 (ROR1) is an onco-embryonic antigen playing an important role in organogenesis (Zhao et al., 2021). Active expression of ROR1 has been detected in a variety of cancer types, including prostate cancer and, studies have revealed the implications of ROR1 expression in tumor cell growth and aggressiveness and its potential as a therapeutic target (Zhang et al., 2012; Zhang et al., 2012; Cui et al., 2016; Zhang et al., 2019). Studies suggest that ROR1's involvement in oncogenesis is done through its activation by

Wnt5A ligand, mediating the non-canonical WNT signaling (Huang et al., 2009; Lee et al., 2018; Yamamoto et al., 2010; Chen et al., 2019; Luo et al., 2020; Sandsmark et al., 2017; Yu et al., 2016; Yu et al., 2017). Non-canonical β-catenin-independent WNT signaling is thought to be involved in the regulation of mechanisms such as cell polarity, proliferation, motility, and migration (Butler & Wallingford, 2017; De, 2012). Observing the unusual activation of ROR1 expression and its involvement in tumor environments, it appeals as a potential therapeutic target against metastatic prostate cancer.

CLIC1 and CLIC1 Inhibitor, IAA94

Chloride intracellular channel protein 1 (CLIC1) is known to be an important biomarker in several cancer types, including prostate cancer (Gururaja Rao et al., 2020; Ummanni et al., 2008; Lee et al., 2010). CLIC1 is expressed in normal adult tissues and performs indispensable physiological functions (Valenzuela et al., 1997; Ulmasov et al., 2007). CLIC1 can appear in two forms: a cytosolic form and a transmembrane one functioning as a chloride channel (Cianci & Verduci, 2021). It has been discovered that CLIC1 is upregulated and is mostly present as a transmembrane protein in tumor cells and, its translocation correlates with tumor aggressiveness and progression (Setti et al., 2013). With the knowledge that chloride ion flux is involved in cell proliferation (Lathrop & Loeb, 1916), CLIC1 is associated with cell proliferation and migration in human prostate cancer cell lines (Tian et al., 2014; Bu & Diehl, 2016). Other studies have revealed that decreased expression (downregulation) of CLIC1 leads to decreased cell migration and invasion in colon cancer, gastric cancer, and glioblastoma (Ma et al., 2012; Wang et al., 2012; Setti et al., 2013; Wang et al., 2014; Li et al., 2018). These same results were obtained upon inhibition of CLIC1 with IAA94 (Zhao et al., 2015). IAA94 was originally designed as a diuretic treatment in 1977, and it is shown to be safe (Woltersdorf et al., 1977; deSolms et al.,

1978). IAA94 was revealed as a chloride channel inhibitor (Landry et al., 1987) and was proven to be effective at inhibiting CLIC1 translocation to the cell membrane (Xu et al., 2016). Since CLIC1 translocation is an undeniable hallmark of cancer progression and metastasis, we propose that by targeting its translocation, we could prevent the tumor from metastasizing. The work presented here will use prostate cancer cell lines expressing CLIC1 and, the small molecule CLIC1 inhibitor, IAA94, will be used to target CLIC1 translocation. However, although IAA94 can inhibit CLIC1 translocation, its specificity remains questionable. In fact, studies have shown that IAA94 is not target-specific, as it can also affect other CLIC proteins: (CLIC3, CLIC4, and CLIC5) (Gururaja Rao et al., 2020; Peretti et al., 2018; Singh, 2010). As a future study, we aim to use new CLIC1 inhibitors that are more target specific to perform the assays. Since IAA94 provides a good structural basis for a CLIC1 inhibitor, it will be used as the starting point for developing new CLIC1 inhibitors that are more target specific to perform the assays. We are working in collaboration here at UCSD with Dr. Dionicio Siegel who is synthesizing the new CLIC1 inhibitors and Dr. Olivia Osborne who is testing the new CLIC1 inhibitors in a Chloride ion flux assay. The main goal is to preserve the ability to inhibit CLIC1 translocation to the membrane and the resulting Chloride ion flux while improving the specificity of the inhibitor and keeping its toxicity level low.

Hypothesis

Docetaxel is currently being used as a chemotherapy drug for advanced prostate cancer and has been proven to be effective to some extent. However, prostate cancer often develops resistance to Docetaxel. We are interested in investigating new pathways that have the potential to overcome this resistance. From preliminary analysis of ours and others, we propose the ROR1

and CLIC1 pathways as new targets for therapies that can work either alone or in combination with Docetaxel to combat prostate cancer. Our goal here was to optimize a cell-based assay technique using the Incucyte live cell analysis to make it a reliable technique to test the effect of therapies on cell proliferation and the cell cycle. We seek to investigate the effect on cell proliferation and cell cycle of Docetaxel treatment in combination with the inhibition of ROR1 or CLIC1 pathways.

CHAPTER 1 METHODS

Cell lines:

The prostate cancer cell lines, PC3, were purchased as frozen vials in 10% DMSO, 90% fetal bovine serum (FBS), from the American Type Culture Collection (ATCC, atcc.org, Manassas, VA). Cells were grown in cell culture according to the recommended protocol in F-12K nutrient media (Kaigh's modification of Ham's F12 medium, Gibco, Thermofisher catalog number 21127022), 10% FBS, 1% penicillin streptomycin, and incubated at 5% CO_2, 37°C. The adherent cells were cultured in vented cap T75 flasks from Corning (catalog number 10144-832) containing 10ml of growth media and placed flat in a CO2 incubator. Prior to each experiment, the adherent cells to be studied were lifted off the plates and dissociated into single cells using 0.25% trypsin (catalog number 25200114). Weekly maintenance of the cells was performed once the cells reached high confluence defined as the adherent cells covering 80-100% of the flask flat surface area. For comparative purposes, PC-3 ROR1 KO and PC-3 Fucci2BL cells were grown at about the same rate (meaning that during the routine maintenance prior to performing an experiment, all the flasks planned for use in the experiment were split to the same cell number of 500,000 cells per T75 flask in 10 ml media.

Limiting Dilution Cloning Series PC3 Fucci2BL and PC3 ROR1KO

The growth media was first removed from the flasks containing the cell lines of interest. About 3ml of Trypsin was added to the flasks, and the flasks were placed in the incubator for 5 minutes. After 5 minutes, 7ml of growth media (F-12K nutrient media, 10% FBS (fetal bovine serum, 1% penicillin streptomycin) was added to each flask, and the cells from the flasks were collected in separate 50ml falcon tubes. The tubes were centrifuged at 1200RPM and 22°C for 5

minutes. After centrifuging the cells, the supernatant was removed. The cells were resuspended in 10ml of 10% FBS/1%Pen-strep F-12K growth media.

Cell counts were performed using 1:1 dilution in trypan blue dye and a hemocytometer. Depending on the cell number, using additional growth media, a dilution for each tube was made to reach a cell density of 5 cells/mL. Once the dilutions were completed for each cell line, 100 µL of the solutions containing the cells were transferred into each well of a 96-well plate (this is the equivalent of 0.5 cells/well, which reduces the probability that each well will have more than one cell). Then, 1000 cells were placed in one of the corner wells of the 96-well plate (this was intended to help focus the microscope as the start of monitoring the cell growth in each well).

After plating 100ul of the cells, we added 100uL conditioned media from the flask the cells came from. The plates were placed back in the incubator undisturbed for 3-4 days. After several days, we checked all the wells and the well containing the 1000 cells was used to help focus the microscope. We took notes of the number of colonies seen in each well and made sure to mark the wells that had one colony growing (these were the wells of interest). Once the cells in the wells of interest had expanded, but before they reached 80-100% maximum confluence, the cells were transferred to a 24-well plate. To collect the cells from the 96-well plate, we added 100ul of trypsin to each well, incubated the plate for 30 seconds, and added 100ul of growth media to transfer the cells from the 96-well plate to separate Eppendorf tubes. Then, 800ul of growth media was added to the Eppendorf tubes, and they were centrifuged for 5 minutes at 3.0 RPM and 22 degrees Celsius. The supernatant was removed, and the cells were resuspended in 1ml growth media, and the cells from each Eppendorf tube were transferred into the 24-well plate. The cell growth in the 24-well plates was also monitored for up to a week, and the cells were transferred into 6-well plate before they reached maximum confluence. Once the cells in

the 6-well plates had expanded, the cells were collected in 50ml falcon tubes containing growth media and aliquot of cells were brought to Dr. Charles Prussak's lab at the Center for Novel Therapeutics, UCSD, where Christopher Oh performed FACS analysis using anti-ROR1 4A5-Alexa 647 antibody –fluorochrome conjugate (for ROR1 expression), and Fucci2BL fluorescent cell cycle markers, hCdt1-mCherry (red fluorescence, G1/G0) and hGem-mVenus (green fluorescence, G2).

Real time cell assays to test with Docetaxel and IAA94

Three clones of each PC3 Fucci and PC3 ROR1KO, which had been selected from FACS analysis, were grown in T75 flasks. On the day of the experiment, each of these clones were plated in 96-well plates at a density of 10,000 cells/well. Using a single pipette of 200ul, the cells were first added in 100ul growth media to the wells. Then, the different concentrations of Docetaxel and IAA94 were added as shown in figures 2.h and 3.g. We placed the plates in the incubator to allow the cells to attach to the bottom of the wells. After about 16 hrs, we started the time course of microscope imaging with the IncuCyte (IncuCyte S3). Cells were imaged every 2 hours for up to 6 days and 10 hours using the IncuCyte Live-Cell Analysis System with data collection by the Incucyte 2020C accompanying software.

Details of Drug Dilutions and Plate set-up

Docetaxel and IAA94 were stored as stock solutions with concentrations of 50uM and 400mM respectively. Dilution series were performed to test 3, 30, 300nM Docetaxel and 20, 40, 100uM IAA94 in 2 separate 96-well plates. The details of the plates' set-up are shown in tables 1 and 2.

Data Analysis

Cell Proliferation (Effect of treatments on Percent Confluence)

To estimate the effect of the drugs on the cell proliferation, the percent confluence from each well was directly extracted from the software embedded in the Incucyte. Since each treatment condition was done in triplicate, the percent confluence corresponding to each treatment condition was derived by calculating the average percent confluence from the 3 wells using excel. Then, the figures for each drug treatment were made, displaying the percent confluence for each treatment condition as time advanced.

Change in percent confluence

To account for the small differences in the starting cell numbers of the wells, we used the percent confluence data to calculate the change in percent confluence from the assay start (scan start).

For each well, we calculated, the ratio of the percent confluence at each time point over the percent confluence of the starting time point (time = 0hr). Then, we calculated the average from the triplicate wells for each treatment condition.

Effect of treatments on the Cell cycle

The green, red, and yellow counts were measured by the IncuCyte software every 2 hours for each well. The data collected were imported, and the average green, red, and yellow counts was calculated for each treatment condition. Then, the percent green, red, and yellow were generated for each treatment condition. The figure for each treatment condition was made, showing the percent green, red, and yellow counts as time advanced and the corresponding cell cycle stage based on the fluorescent label from Fucci2BL Cell Cycle tracker.

Fucci Lentiviral Transduction and Fluorescent Digital Microscope Imaging

The *Fucci2 BL* bicistronic fluorescent, ubiquitination-based cell cycle indicator reporter system can show four cell cycle phases: G_1/G_0 by red fluorescence, G_1/S by yellow fluorescence and G_2/M by green fluorescence and G_0 by bright red fluorescence. Both mVenus-hGem (1/110) and mCherry-hCdt1 (30/120) were subcloned into a pCDHEF1α-T2A lentiviral expression vector (Pineda *et al* 2016 Sci Rep). Fucci2BL was a generous gift from Dr. Catriona Jamieson, UCSD which was stably transduced into prostate cancer cell lines PC3 (by Michelle Muldong) and PC3_ROR1KO (by Evodie Koutouan) as described below according to the recommendations of Dr. Gabriel Pineda in Dr. Catriona Jamieson's laboratory.

The PC3 and PC3 ROR1KO cells were seeded at a density of 50,000cells/well in 100uL of growth media into flat-bottom Corning 96-well plates. Then, the Fucci lentivirus vector used to produce non-replicating viral particles (Pineda *et al* 2016 Sci Rep), were added to each well at increasing multiplicity of infection (MOI). Specifically, increasing amounts of virus were added as: 0.5, 0.75, 1.0, 1.5, 2.0 microliters per well. The plate was left undisturbed in the incubator for 72hrs. After 72hrs, the media from each well was removed, and the adherent cells were washed with 200 ul growth media twice. Fresh growth media (200 ul) was added to the wells, and images of the wells were taken using a Keyence microscope (Keyence Corporation of America, Itasca, IL) and cells with red, green, and yellow fluorescence. Cells that showed green, red and/or yellow fluorescence and were thus, positive for Fucci live cell cycle tracker expression, were expanded for cryopreservation and experiments. For clarification on the timeline, the transduction of PC3 cells was done before the set of cell-based assays described in this report, while the transduction of the PC3 ROR1KO was performed after the limited dilution cloning described above.

CHAPTER 2 RESULTS

Optimization of Real time Cell-based Incucyte Assay

A systematic approach to optimization of the real time, live cell 96-well proliferation assay using the Incucyte S3 is shown in Figure 1.a. Parameters that were optimized were:

- Cell number plated per well to measure proliferative growth curve accurately and reproducibly.
- Cells were plated at same cell number in the cells split prior to plating for the assay to ensure starting with cells that are in proliferating, log phase of growth to minimize lag phase.
- Limited dilution cloning to maximize homogeneity of cells and assay reproducibility.

Limiting Dilution Cloning and FACS Analysis

After the performance of the limited dilution cloning series and the expansion of the clones, we proceeded onto FACS analysis to select the purest populations of PC3 Fucci and PC3 ROR1KO cells. Twelve clones of PC3 Fucci and five clones of PC3 ROR1KO were analyzed through FACS. After the analysis, we selected four clones of PC3 Fucci and three clones of PC3 ROR1KO as indicated by the red arrows in Figure 1.b. The PC3 ROR1KO clones were selected by looking at the ROR1 expression of the cells. We were interested in having pure PC3 ROR1KO cells, so we selected the clones which did not show any ROR1 expression. Regarding PC3 Fucci clones, we selected the ones which had high ROR1 expression and good Fucci2BL expression level. Figure 1.c shows the selection of PC3 Fucci clones based on Fucci2BL expression level.

1. Effect of Docetaxel and IAA94 on PC3 and PC3 ROR1KO Cell Proliferation

a.) Effect of Docetaxel on PC3 Fucci Cell Proliferation

The impact of Docetaxel on the cell proliferation of PC3 Fucci cells was measured using the live cell imaging of the Incucyte. Scans of the wells were taken every two hours and the percent confluence was obtained from the Incucyte software. The graphs in Figures 2.a, 2.b, and 2.c were generated using these numbers. The obtained results revealed that the proliferation of the cells was, to some extent, inhibited by Docetaxel in a dose-dependent manner. Treatment with 300nM Docetaxel was shown to have the greatest impact on the PC3 Fucci cell proliferation. Depending on the clones, we observed a growth plateau in the range of 47% - 77% confluence compared to a range of 99-98%% confluence for untreated and vehicle-treated. PC3 Fucci clone 4 was the most affected among all the three clones that were used in this assay. To account for the small differences in the starting cell numbers of the wells, we used the percent confluence data to calculate the change in percent confluence from the assay start (scan start). As observed in the figure, the lines in all the treatment conditions started to reach a plateau at about the same time (at about 80 hours after the scans started). These observations were consistent among the 3 clones of PC3 Fucci cells used for this experiment. Overall, increasing concentrations of docetaxel produced a decrease in the rate at which the cells were expanding, causing the cells to reach a lower growth plateau. These results show the effectiveness of Docetaxel at inhibiting or slowing down the proliferation of PC3 Fucci cells.

b.) Effect of Docetaxel on Proliferation of PC3 ROR1 Knock Out (KO) cells

Lower final levels of cell culture confluence were observed for the PC3 ROR1KO cells that were treated with Docetaxel (Figures 2.d, 2.e, 2.f), as compared to the results seen above with PC3

Fucci cells. Under treatment with 300nM, 30nM, and 3nM Docetaxel, PC3 ROR1KO clone 1 reached a growth plateau at 67.89%, 56.97%, and 79.71% confluence level, respectively. In the same manner, PC3 ROR1KO clone 2 cells reached a growth plateau at 39.33%, 48.67%, and 58.52% confluence levels, respectively, and PC3 ROR1KO clone 3 reached a growth plateau at 31.64%, 31.44%, and 52.68% confluence levels. On the other hand, the untreated PC3 ROR1KO cells for clone 1, clone 2, and clone 3 reached a growth plateau at 96.68%, 98.83%, and 85.31% confluence levels respectively. These results showed that the knockdown of ROR1 combined with Docetaxel treatment had a greater inhibition of the cell proliferation of the PC3 prostate cancer cells. Interestingly, just by looking at the percent confluence reached in the growth plateau, the untreated PC3 Fucci and untreated PC3 ROR1KO cells did not seem to show a big difference in cell proliferation. However, looking closely at the raw measurements from the Incucyte, we could see that most of the PC3 Fucci clones reached a high confluence level (about 90%) earlier than PC3 ROR1KO cells, except for PC3 ROR1 KO clone 2, which started to reach confluence levels at an earlier time. Overall, Docetaxel had a more dramatic impact on the cell proliferation of the PC3 ROR1KO cells (Figure 2.g). We could conclude that the absence of the ROR1 gene affected the growth of our PC3 cells and made the cells more susceptible to Docetaxel treatment.

c.) Effect of the small molecule CLIC1 inhibitor, IAA94, on Cell Proliferation

Unlike the treatment of the cells with Docetaxel, the proliferation of PC3 Fucci cells treated with IAA94 did not exhibit any difference compared to the untreated PC3 Fucci cells or PC3 Fucci cells treated with the vehicle (100% ethanol). As seen from the graphs (Figures 3.a, 3.b, and 3.c), the wells in the different treatment conditions had the same confluence level. Indeed, the cells in the different treatment conditions reached a growth plateau at the same time, and this

plateau was caused by high confluence levels, revealing that IAA94 did not have any inhibiting effect on cell proliferation. The same lack of an effect of IAA94 on proliferation was observed for PC3 ROR1KO cells (Figures 3.d, 3.e, 3.f). In sum, our assays performed on PC3 Fucci and PC3 ROR1KO cells showed that treatment with IAA94 was not successful at inhibiting cell proliferation.

2. Effect of Docetaxel and CLIC1 Inhibitor on the Cell Cycle Prostate Cancer Cells – PC3 Fucci

a.) Effect of Docetaxel

The effect of Docetaxel on the cell cycle was next measured in real time using the live cell cycle tracker Fucci2BL, which makes the cells fluoresce green, red, or yellow depending on their cell cycle stage. Green fluorescence is an indicator that the cell is in G2 phase. Red indicates that the cell is in G1 or G0, and yellow (green + red) indicates the cell is in S phase (figure 4.a). Using the Incucyte, the green, red, and yellow counts for each well were measured every two hours, and the percent green, red and yellow were calculated. From these numbers, we were able to make a graph showing the percentage of green, red, and yellow fluorescence in each well for the different treatment conditions. As shown by the results, we observed dramatic shifts in the percentage of green (G2 phase indication) vs. red (G1/G0 phase indication) fluorescence comparing the untreated wells to the ones treated with Docetaxel (figures 4.b, 4.c, 4.d).
We observed some differences within the graphs' shape of the clones, but we were able to clearly see that Docetaxel influences the cell cycle of PC3 cells. Upon treatment with 300nM and 30nM Docetaxel on PC3 Fucci clone 2 and 4, there was a higher percentage of red fluorescence for an extended time, which indicates that the cells seemed to remain in the G0/G1 phase during that period (figures 4.c and 4.d). Then, we could observe that around the interval of 100hrs –

120hrs, there was an inversion in the percentage of green vs. red fluorescence. Higher percentage of green fluorescence was detected, which indicates that the cells went into G2 phase. Thinking back upon the results on cell proliferation (Figures 2.a, 2.b, and 2.c), we could see that the cells in the docetaxel treated wells remained in a growth plateau (at low confluence levels) during that period. The same observations were made for PC3 Fucci clone 1 except that the inversion in the percentage of green vs. red fluorescence occurred earlier. Thus, the data provides evidence of a *G2 phase arrest* in the cell cycle for the PC3 cells that were treated with Docetaxel, in contrast with the G1 arrest of untreated or vehicle-treated cells at the plateau of proliferative growth.

b.) Lack of Effect from CLCI1 Inhibitor, IAA94

As might be suspected from our data looking at the effect of IAA94 on cell proliferation, we found that there was no evidence that IAA94 had an impact on the cell cycle phases of the PC3 Fucci cells (figures 5.a, 5.b, 5.c). Specifically, there was not an obvious difference in the curves comparing the IAA94-treated cells to the untreated cells. The cells treated with IAA94, and the untreated ones had a cell cycle arrest in G1/G0, which coincided with high confluence levels for all the PC3 Fucci clones, looking at the timeline.

3. PC3 ROR1 KO Fucci Lentiviral Transduction and Fluorescent Microscope Imaging

We transduced PC3 ROR1 KO knock out cells using the live cell cycle tracker Fucci2BL, which makes the cells fluoresce green, red, or yellow depending on their cell cycle stage. To test the success of the transduction, each well was observed using the Keyence microscope, with which we can take microscopic images of fluorescent cells. We successfully transduced the PC3-ROR1KO cells with the Fucci2BL cell cycle tracker lentivirus. We could observe an increased level of fluorescence as an increased amount of Fucci Lentivirus was added to the wells. As

expected, our negative control (PC3 ROR1 KO cells in the well without addition of the Fucci2BL Lentivirus), did not have any red, green, or yellow fluorescence. This was confirmation that the fluorescent microscope has consistent data. We now have all the cell lines needed to complete further experiments to analyze effects of docetaxel and IAA94 on cell cycle of PC3 cells lacking ROR1 expression.

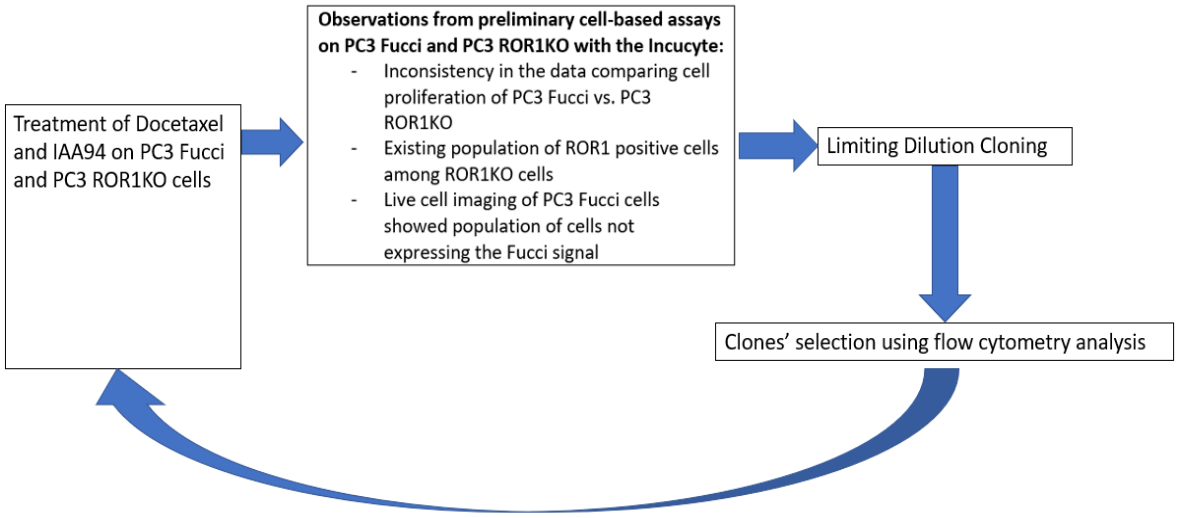

Figure 1.a: **Optimization of Cell-Based Assay**

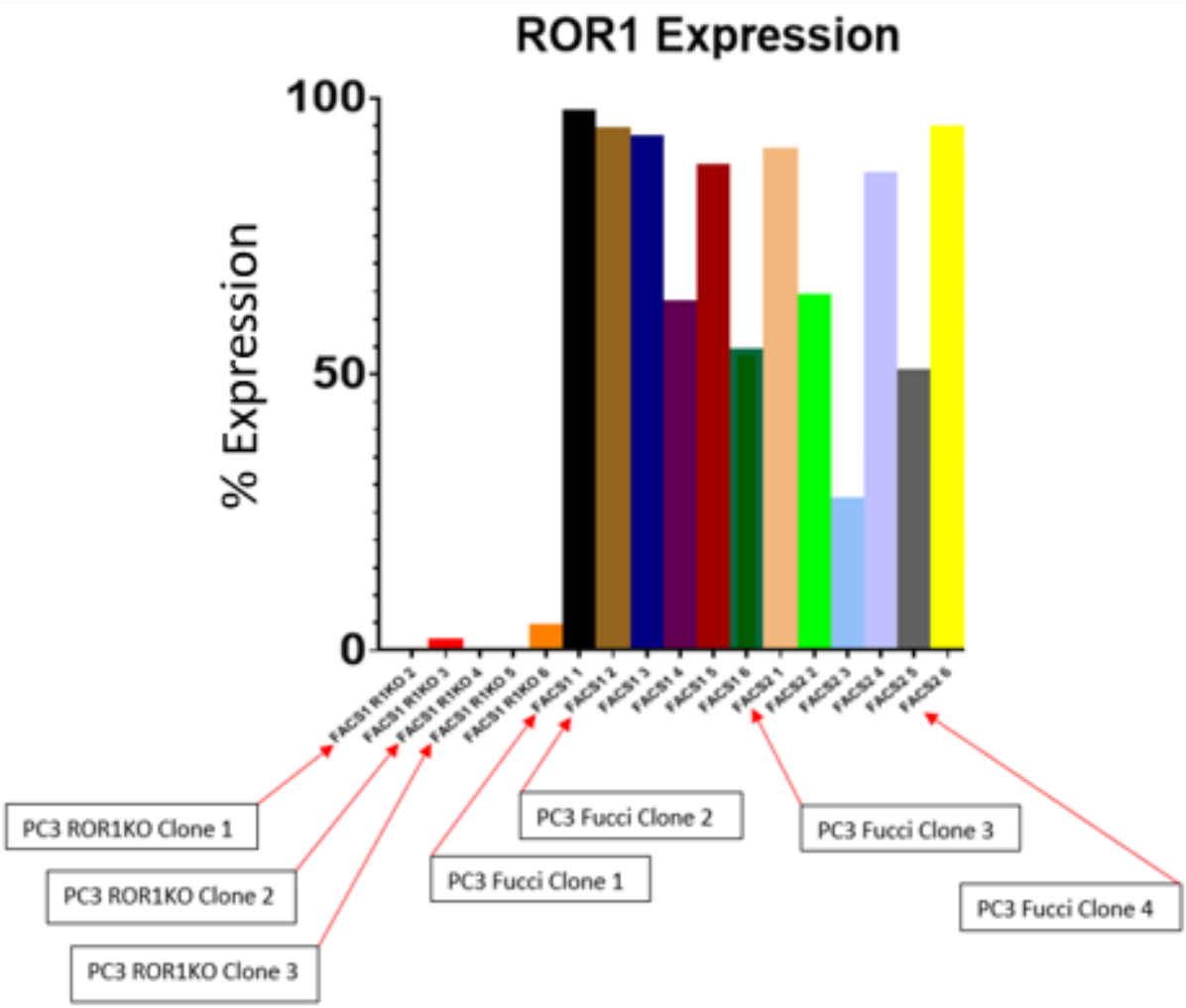

Figure 1.b: **Selection of PC3 ROR1KO and PC3 Fucci clones after limiting dilution series based on their ROR1 expression**

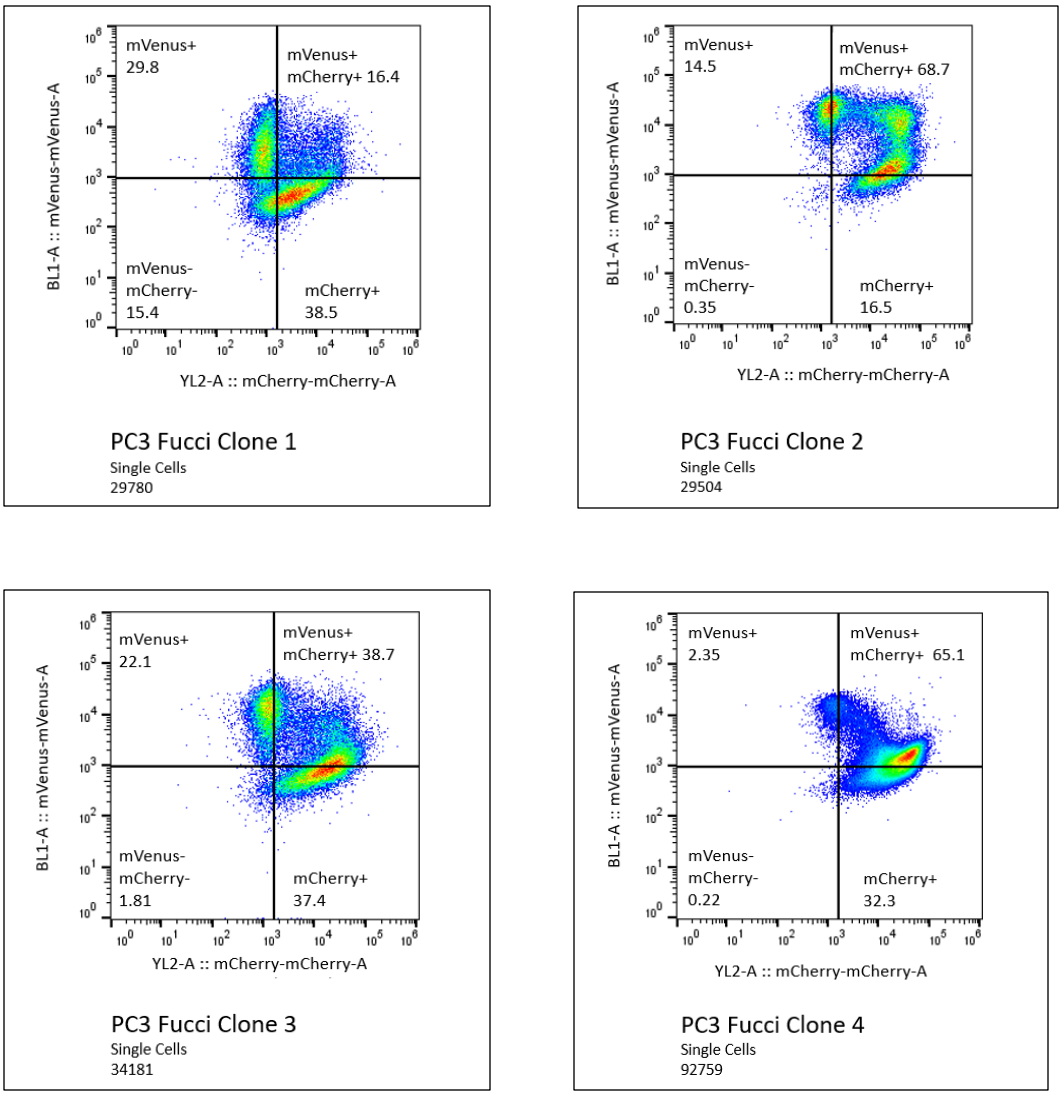

Figure 1.c: **Selection of PC3 Fucci clones after limiting dilution series based on Fucci2BL expression**

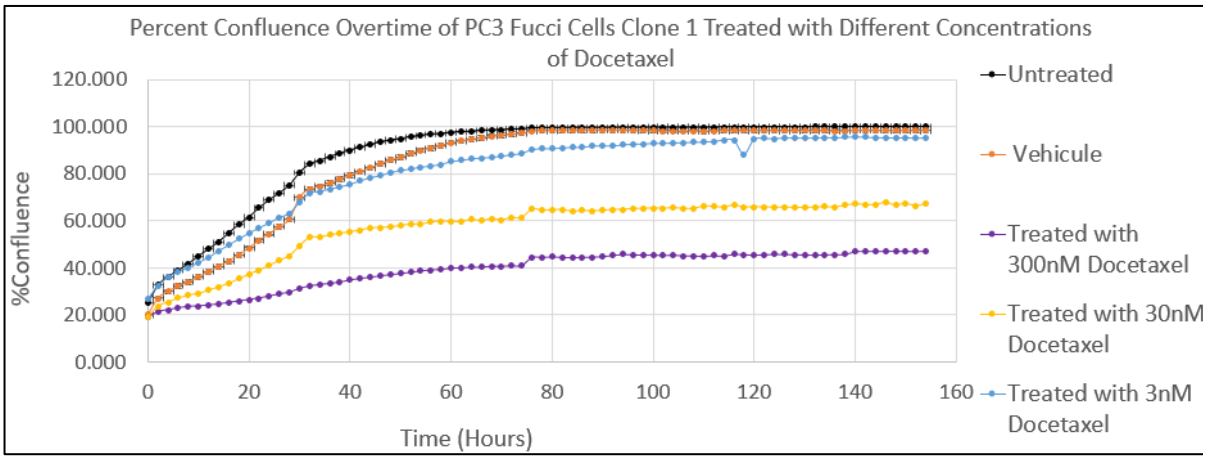

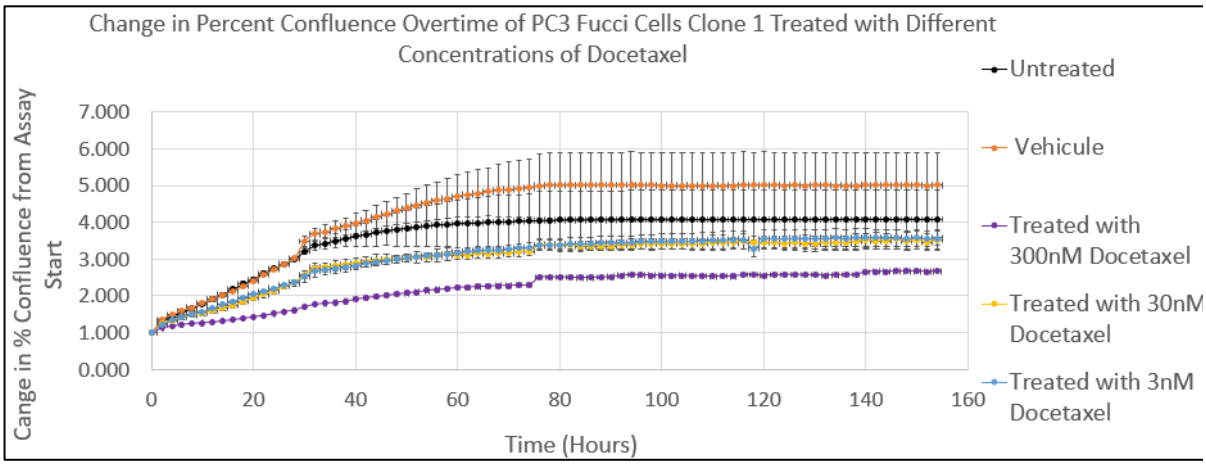

Figure 2.a: **Treatment with the prostate cancer chemotherapy drug, Docetaxel, results in dose-dependent inhibition of proliferation in PC3 cells clone 1 in real time cell imaging analysis.** After the cells were seeded into the 96 well plate, different condition treatments were added in triplicates. The scans in the IncuCyte started about 16 hours after the cells were added into the wells. The images were taken every two hours for a total of 154 hours. The percent confluence of each well was generated through the software embedded in the IncuCyte. The graph (top panel) shows the percent confluence of the wells as time advanced. The graph (bottom panel) shows the change in the percent confluence of the wells from the starting point of the scans.

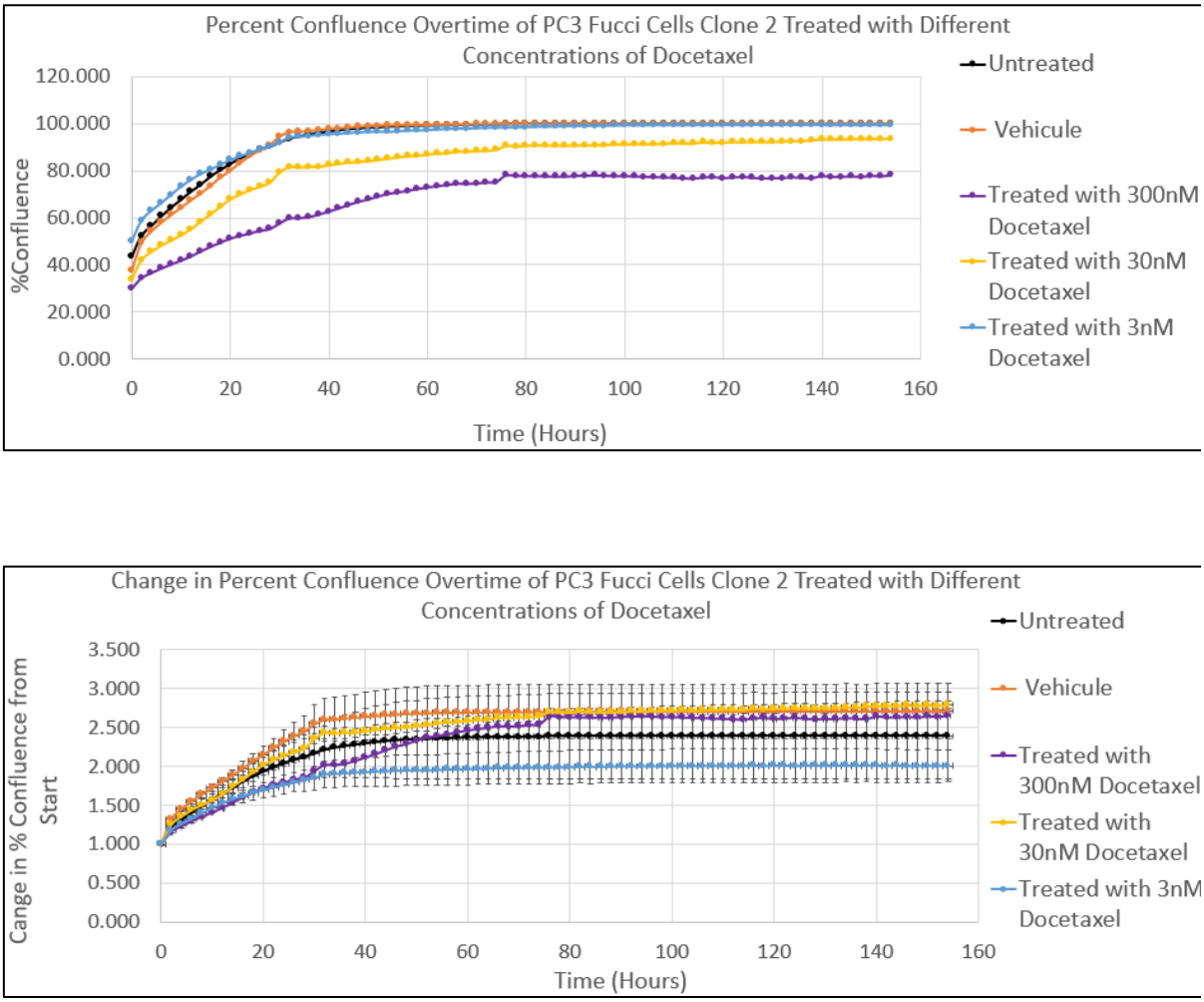

Figure 2.b: **Treatment with the prostate cancer chemotherapy drug, Docetaxel, results in dose-dependent inhibition of proliferation in PC3 cells clone 2 in real time cell imaging analysis.** After the cells were seeded into the 96 well plate, different condition treatments were added in triplicates. The scans in the IncuCyte started about 16 hours after the cells were added into the wells. The images were taken every two hours for a total of 154 hours. The percent confluence of each well was generated through the software embedded in the IncuCyte. The graph (top panel) shows the percent confluence of the wells as time advanced. The graph (bottom panel) shows the change in the percent confluence of the wells from the starting point of the scans.

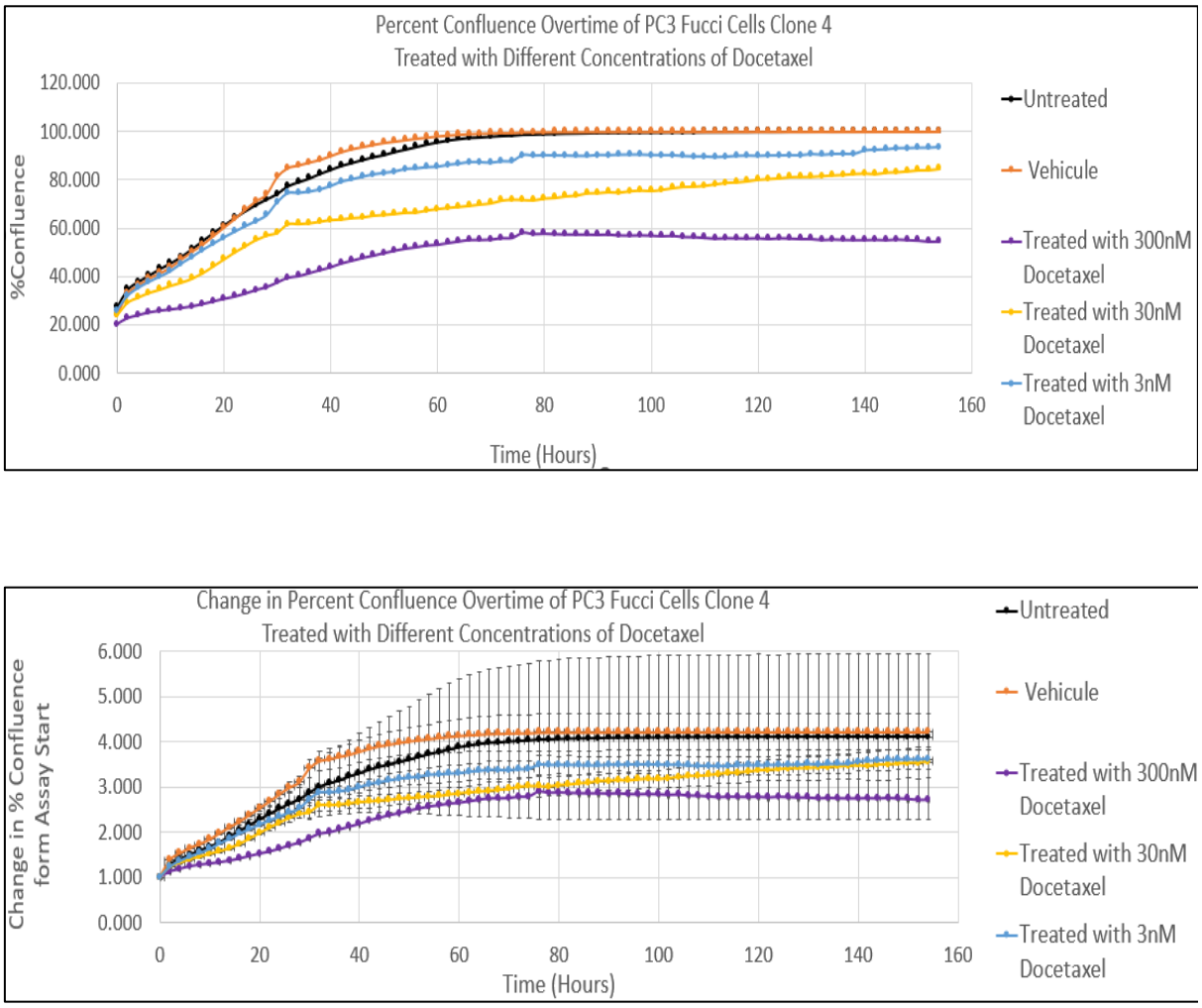

Figure 2.c: **Treatment with the prostate cancer chemotherapy drug, Docetaxel, results in dose-dependent inhibition of proliferation in PC3 cells clone 4 in real time cell imaging analysis.** After the cells were seeded into the 96 well plate, different condition treatments were added in triplicates. The scans in the IncuCyte started about 16 hours after the cells were added into the wells. The images were taken every two hours for a total of 154 hours. The percent confluence of each well was generated through the software embedded in the IncuCyte. The graph (top panel) shows the percent confluence of the wells as time advanced. The graph (bottom panel) shows the change in the percent confluence of the wells from the starting point of the scans.

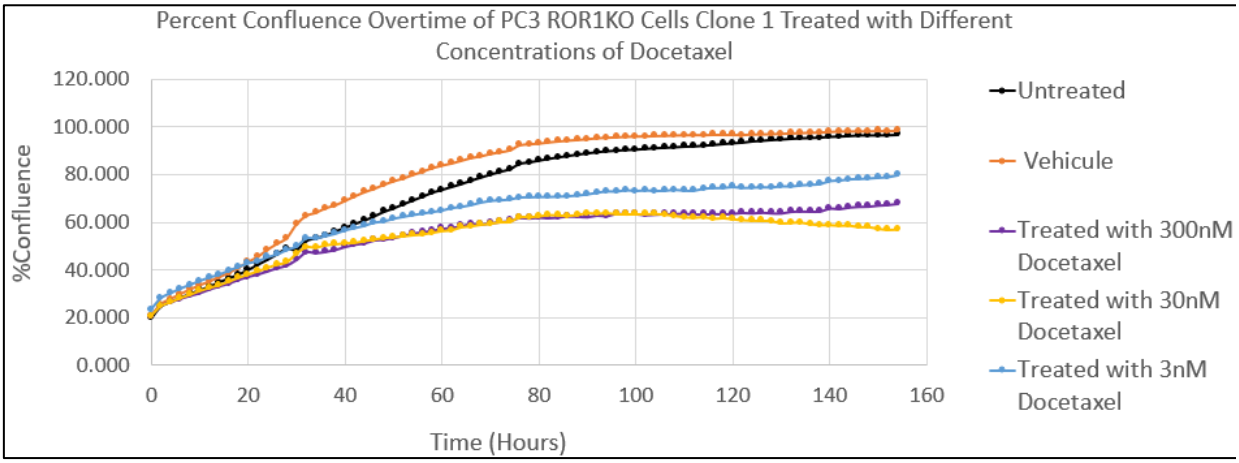

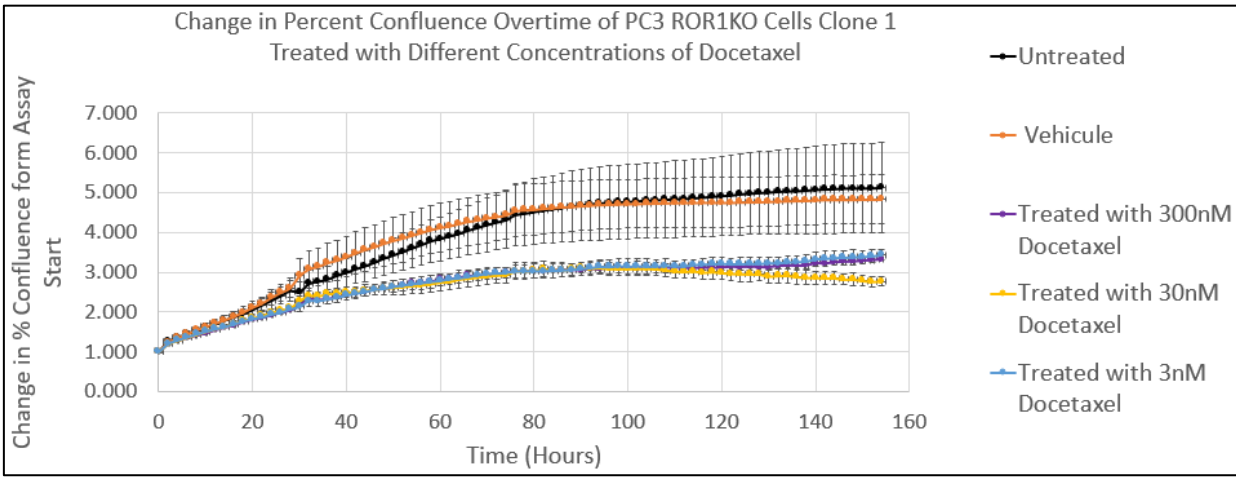

Figure 2.d: **Treatment with the prostate cancer chemotherapy drug, Docetaxel, results in dose-dependent inhibition of proliferation in PC3 ROR1KO clone 1 in real time cell imaging analysis.** The graph (top panel) shows the percent confluence of the wells as time advanced. The graph (bottom panel) shows the change in the percent confluence of the wells classified into the different treatment conditions.

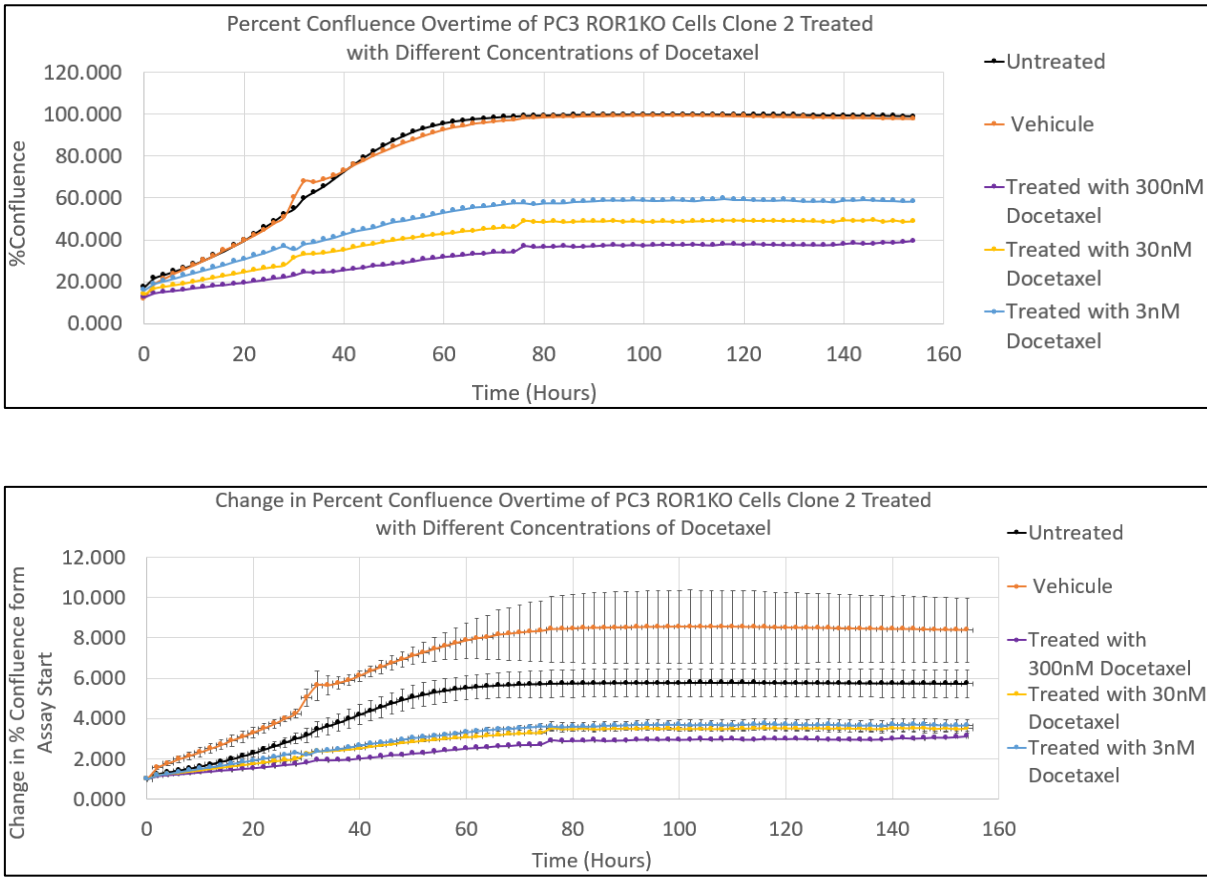

Figure 2.e: **Treatment with the prostate cancer chemotherapy drug, Docetaxel, results in dose-dependent inhibition of proliferation in PC3 ROR1KO clone 2 in real time cell imaging analysis.** The graph (top panel) shows the percent confluence of the wells as time advanced. The graph (bottom panel) shows the change in the percent confluence of the wells classified into the different treatment conditions.

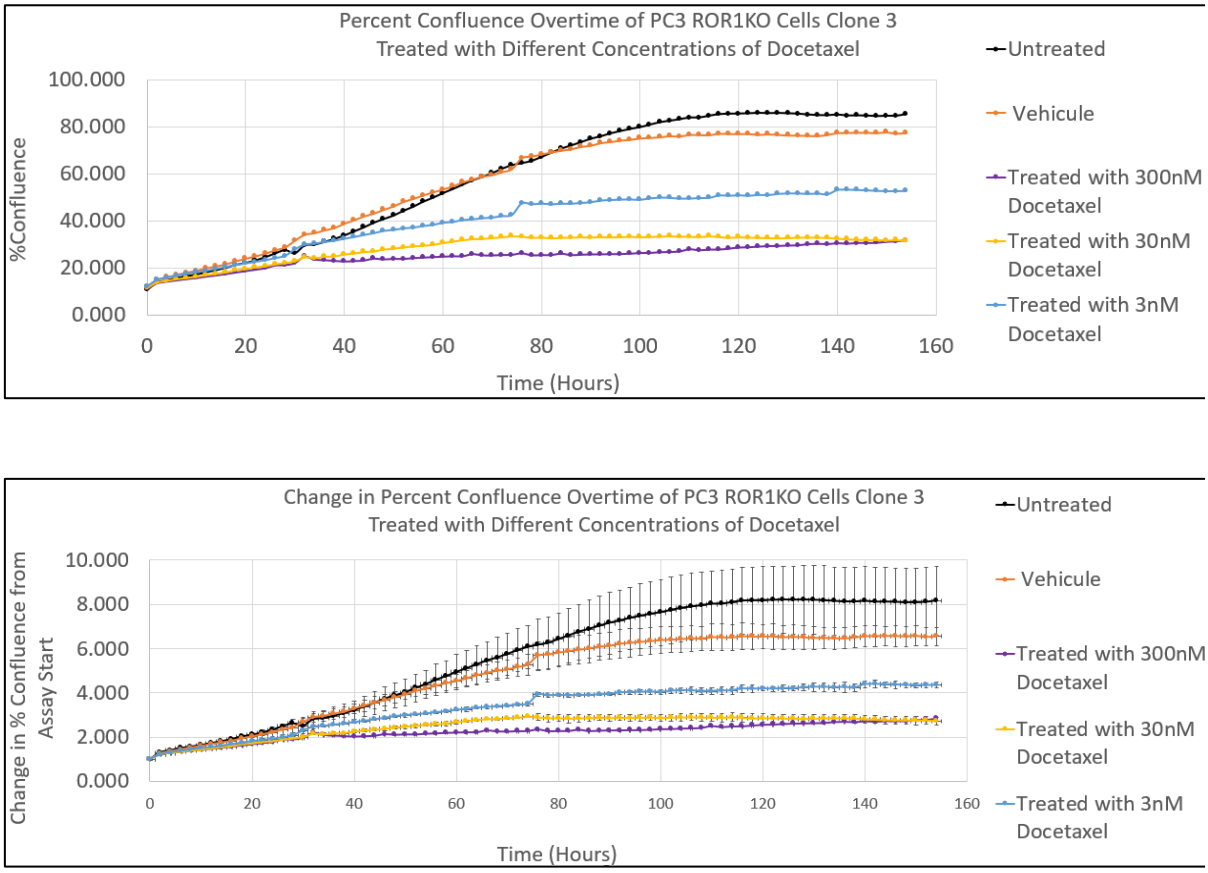

Figure 2.f: **Treatment with the prostate cancer chemotherapy drug, Docetaxel, results in dose-dependent inhibition of proliferation in PC3 ROR1KO clone 3 in real time cell imaging analysis.** The graph (top panel) shows the percent confluence of the wells as time advanced. The graph (bottom panel) shows the change in the percent confluence of the wells classified into the different treatment conditions.

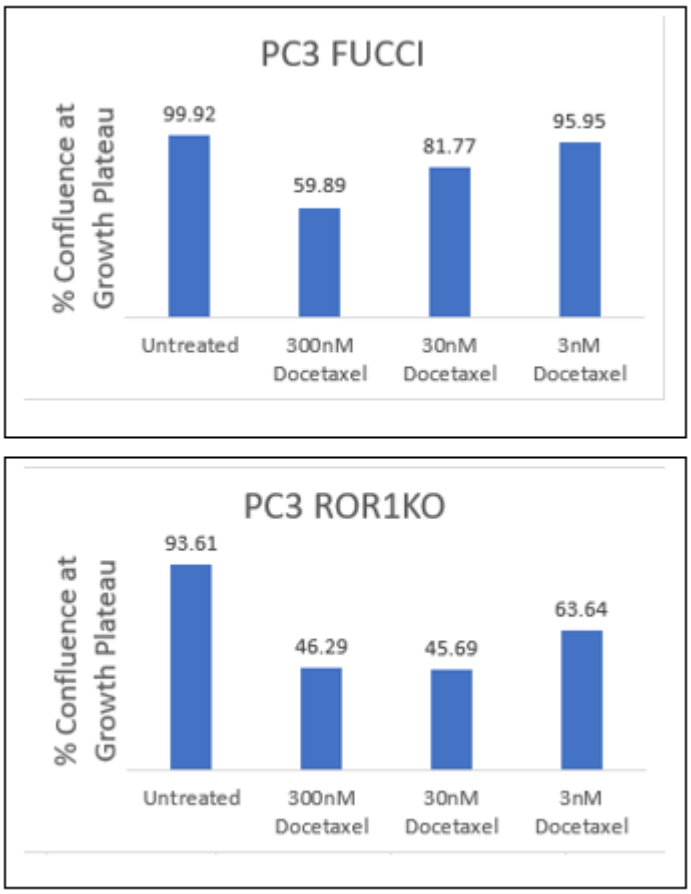

Figure 2.g: **Percent Confluence at Growth plateau of PC3 cells vs PC3 ROR1KO when treated with chemotherapy drug, Docetaxel shows the increased sensitivity PC3 ROR1KO cells to Docetaxel treatment**

Docetaxel 3, 30, 300 nM

	1	2	3	4	5	6	7	8	9	10	11	12
A	Fucci-1	untreat.		ROR1KO	-1	untreat.	Fucci-1	vehicle		ROR1KO	-1	vehicle
B	Fucci-2			ROR1KO	-2		Fucci-2			ROR1KO	-2	
C	Fucci-3			ROR1KO	-3		Fucci-3			ROR1KO	-3	
D	Fucci-1	Doc 300		ROR1KO	-1	Doc 300	Fucci-1	-1	Doc 30	ROR1KO	-1	Doc 30
E	Fucci-2			ROR1KO	-2		Fucci-2	-2		ROR1KO	-2	
F	Fucci-3			ROR1KO	-3		Fucci-3	-3		ROR1KO	-3	
G	Fucci-1	Doc 3		Fucci-3	Doc 3		ROR1KO	-1	Doc 3	ROR1KO	-3	Doc 3
H	Fucci-2			media			ROR1KO	-2		media		

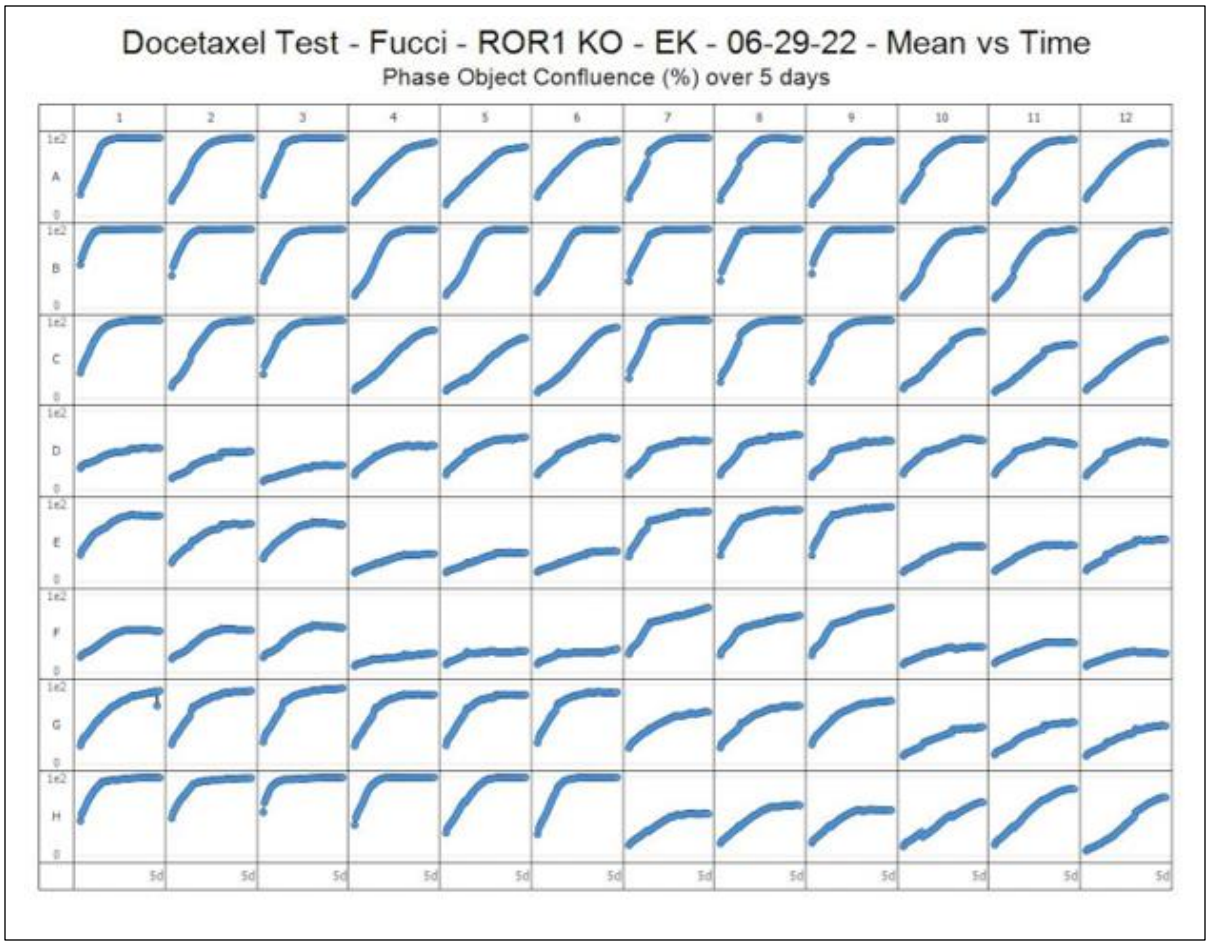

Figure 2.h: **96-well plate set up and percent confluence micrographs of PC3 Fucci clone 1, clone 2, and clone 4 treated with Docetaxel, in real time cell imaging analysis.** The top panel shows the 96-well plate set up for the treatment of PC3 Fucci and PC3 ROR1KO cells with Docetaxel. The bottom panel shows micrographs of the percent confluence as time advanced in all 96 wells. The percent confluence of each well was generated through the software embedded in the Incucyte. The graphs show the percent confluence of the wells as time advanced in all 96 wells.

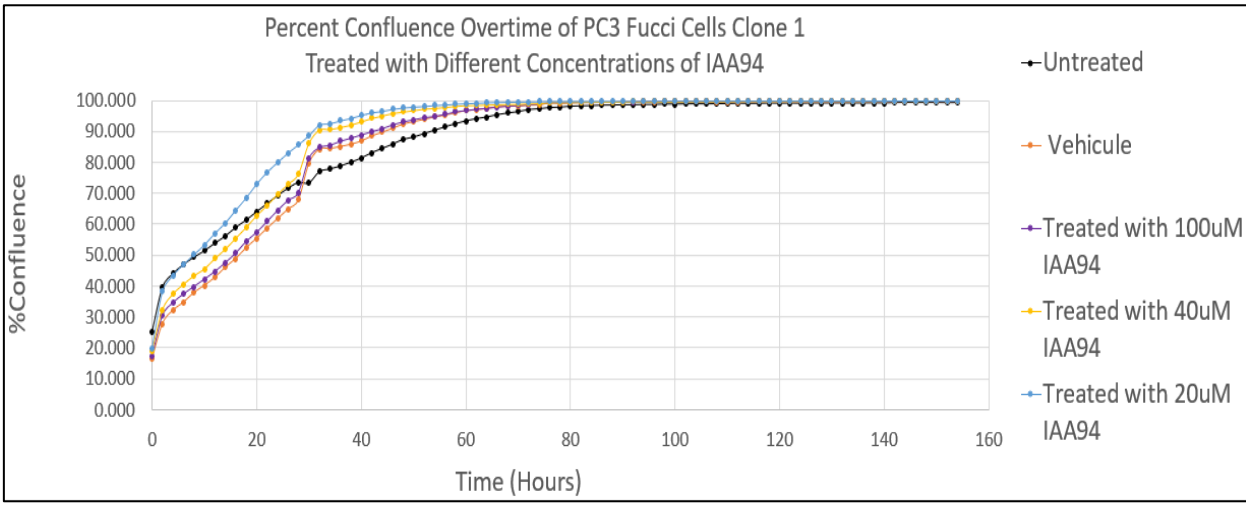

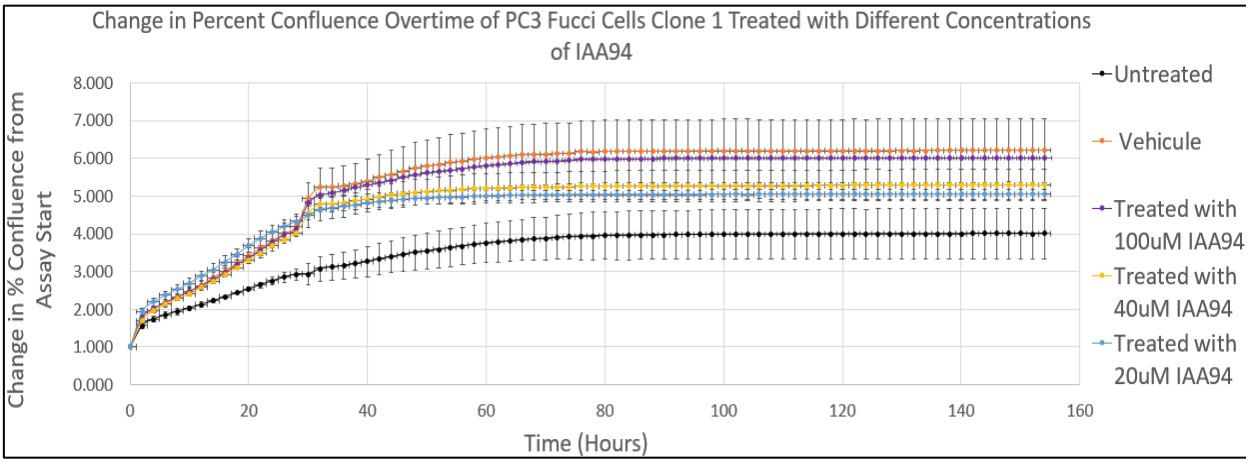

Figure 3.a: **Treatment with CLIC1 inhibitor, IAA94, on PC3 Fucci clone 1 in real time cell imaging analysis.** The graph (top panel) shows the percent confluence of the wells as time advanced. The graph (bottom panel) shows the change in the percent confluence of the wells classified into the different treatment conditions.

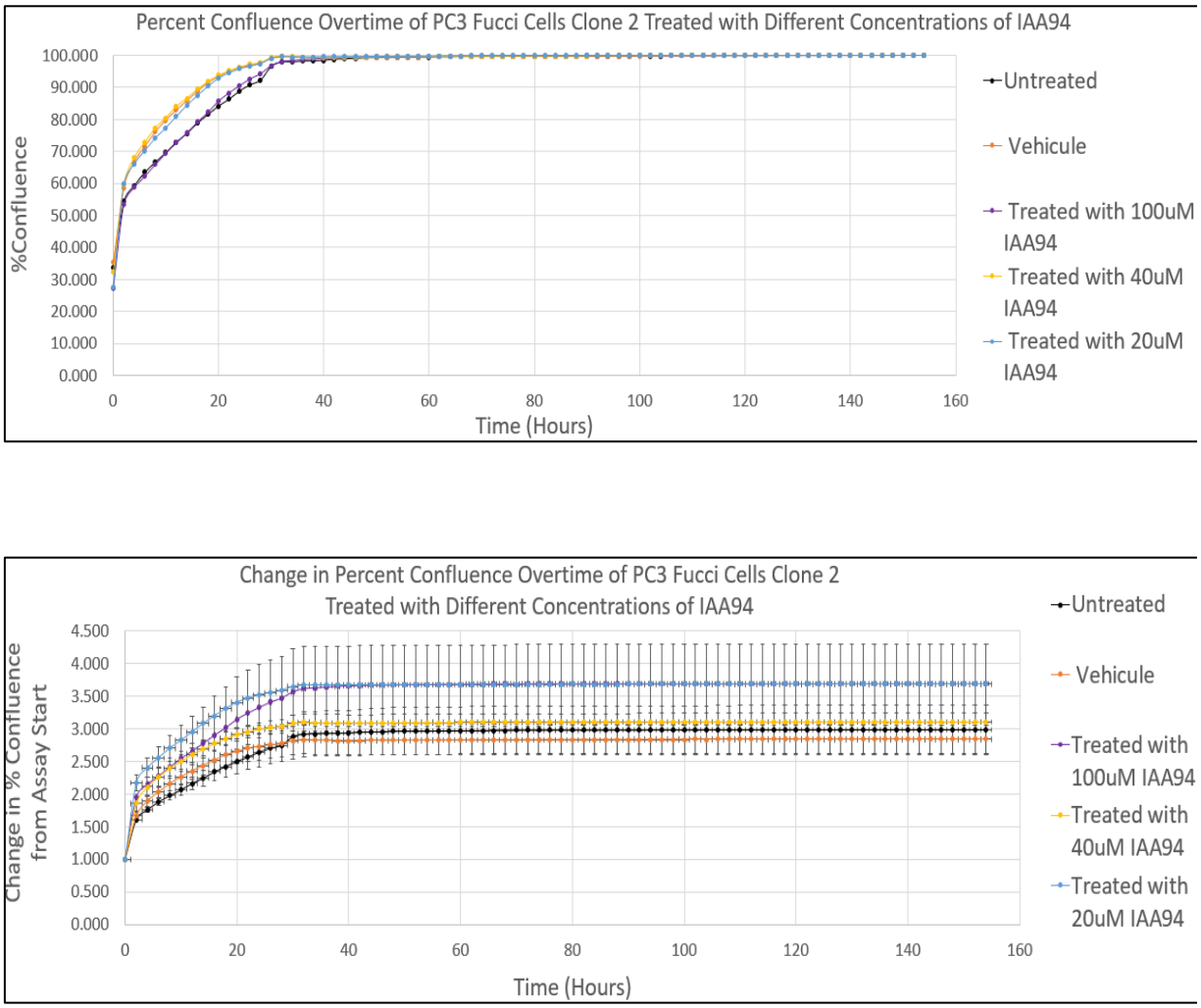

Figure 3.b: **Treatment with CLIC1 inhibitor, IAA94, on PC3 Fucci clone 2 in real time cell imaging analysis.** The graph (top panel) shows the percent confluence of the wells as time advanced. The graph (bottom panel) shows the change in the percent confluence of the wells classified into the different treatment conditions.

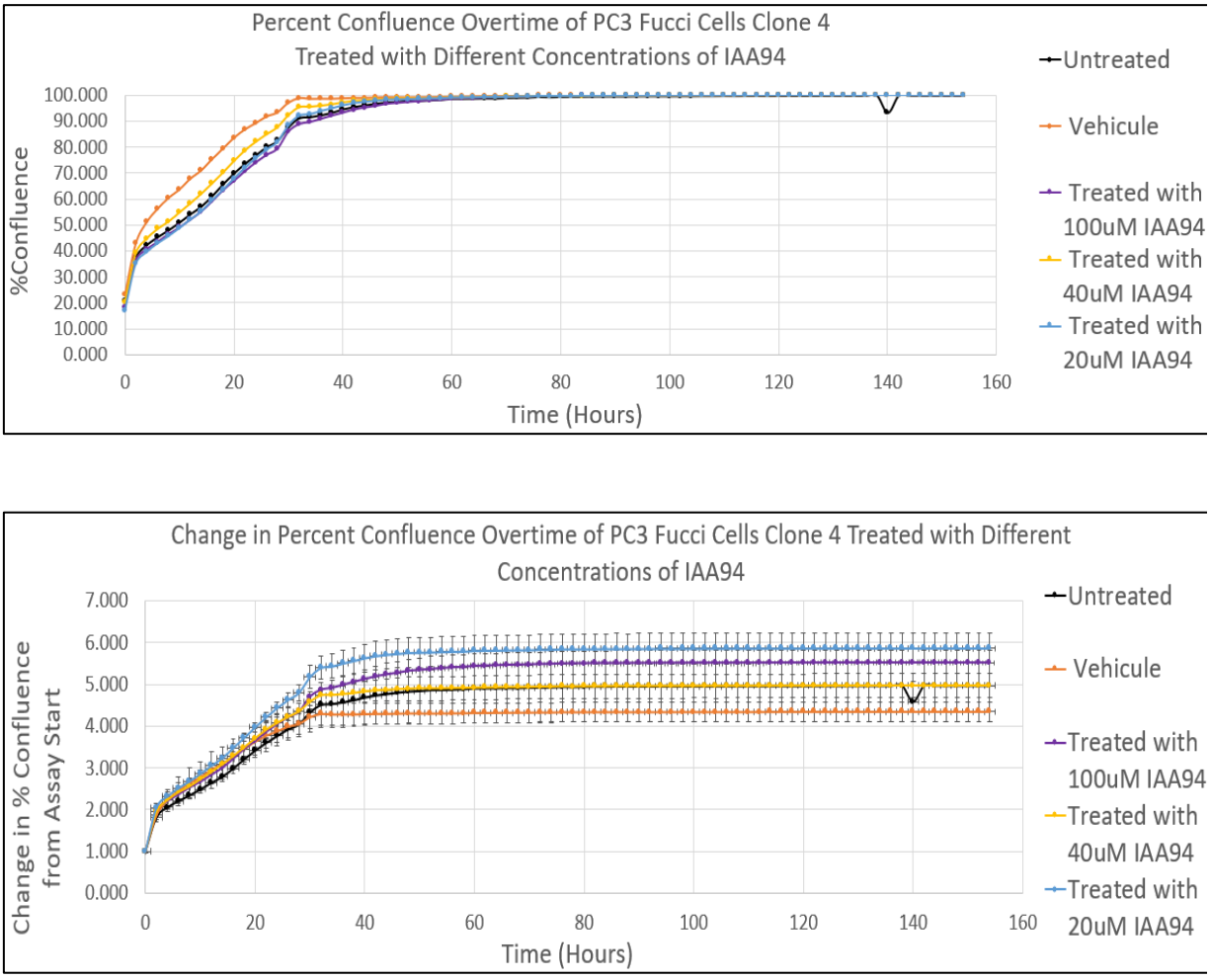

Figure 3.c: **Treatment with CLIC1 inhibitor, IAA94, on PC3 Fucci clone 4 in real time cell imaging analysis.** The graph (top panel) shows the percent confluence of the wells as time advanced. The graph (bottom panel) shows the change in the percent confluence of the wells classified into the different treatment conditions.

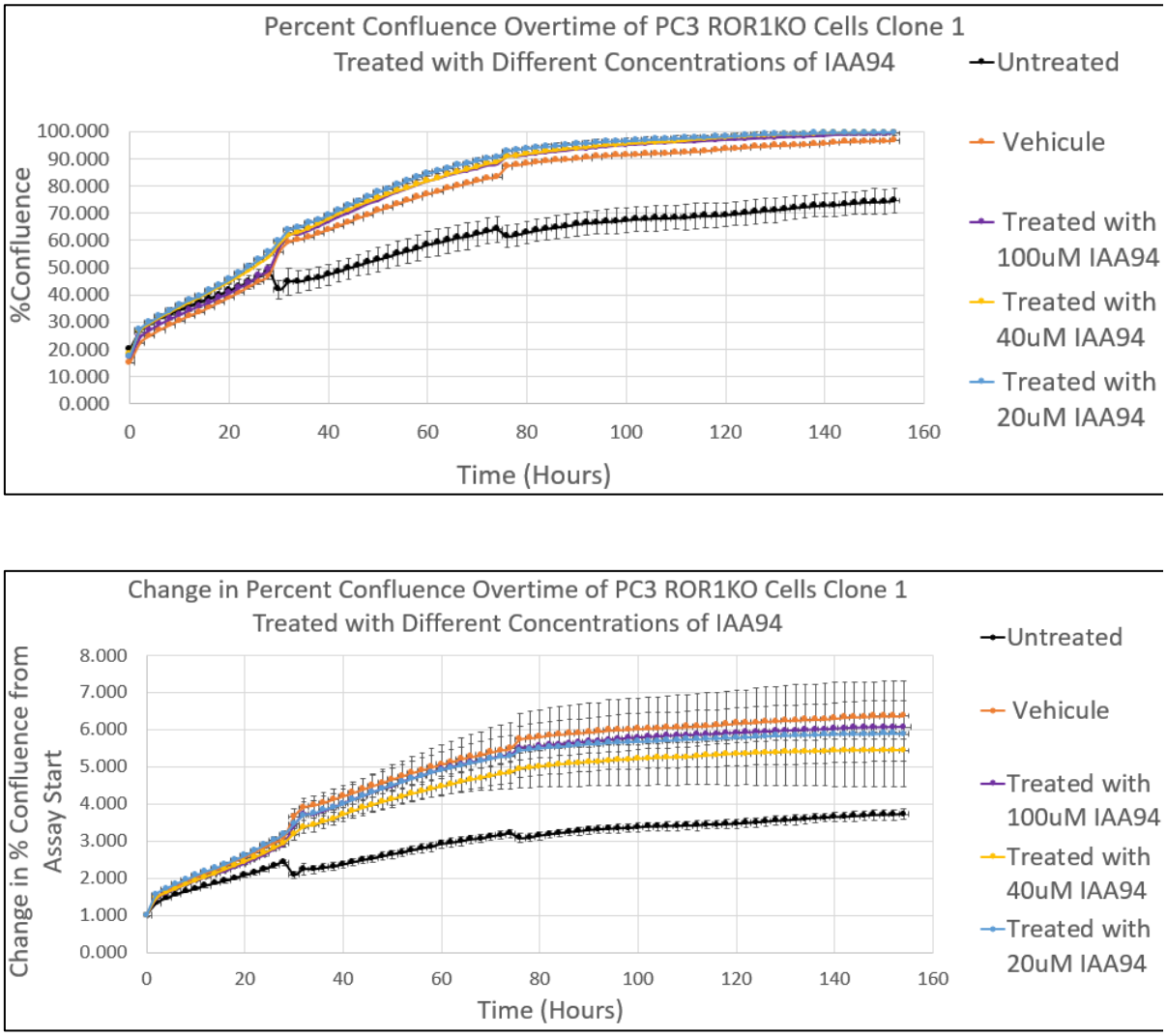

Figure 3.d: **Treatment with CLIC1 inhibitor, IAA94, on PC3 ROR1KO clone 1 in real time cell imaging analysis.** The graph (top panel) shows the percent confluence of the wells as time advanced. The graph (bottom panel) shows the change in the percent confluence of the wells classified into the different treatment conditions.

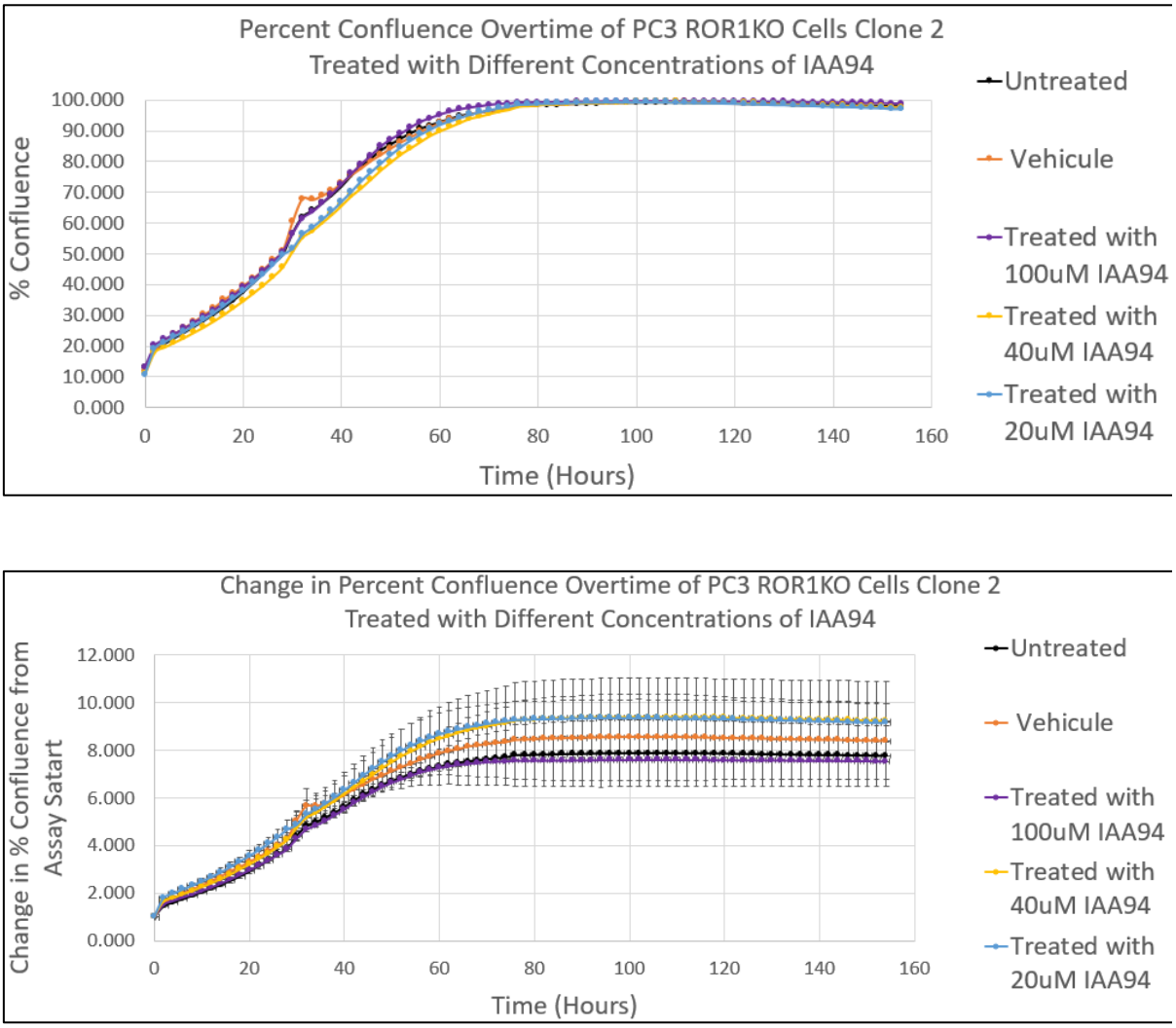

Figure 3.e: **Treatment with CLIC1 inhibitor, IAA94, on PC3 ROR1KO clone 2 in real time cell imaging analysis.** The graph (top panel) shows the percent confluence of the wells as time advanced. The graph (bottom panel) shows the change in the percent confluence of the wells classified into the different treatment conditions.

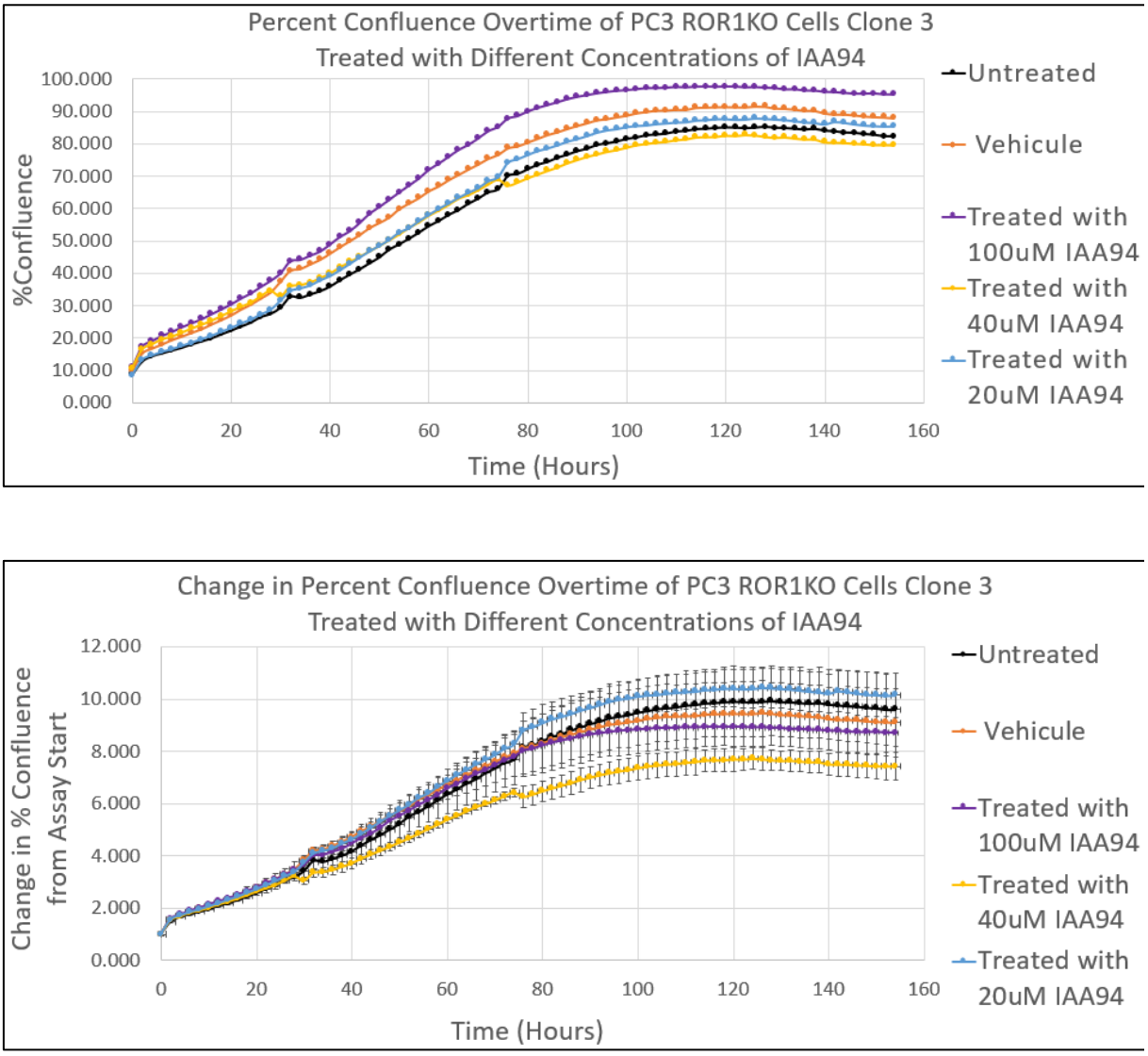

Figure 3.f: **Treatment with CLIC1 inhibitor, IAA94, on PC3 ROR1KO clone 3 in real time cell imaging analysis.** The graph (top panel) shows the percent confluence of the wells as time advanced. The graph (bottom panel) shows the change in the percent confluence of the wells classified into the different treatment conditions.

IAA94 20,40,100 uM

	1	2	3	4	5	6	7	8	9	10	11	12
A	Fucci-1	untreat.		ROR1KO	-1	untreat.	Fucci-1	vehicle		ROR1KO	-1	vehicle
B	Fucci-2			ROR1KO	-2		Fucci-2			ROR1KO	-2	
C	Fucci-3			ROR1KO	-3		Fucci-3			ROR1KO	-3	
D	Fucci-1	IA 100		ROR1KO	-1	IA 100	Fucci-1	-1	IA 40	ROR1KO	-1	IA 40
E	Fucci-2			ROR1KO	-2		Fucci-2	-2		ROR1KO	-2	
F	Fucci-3			ROR1KO	-3		Fucci-3	-3		ROR1KO	-3	
G	Fucci-1	IA 20		Fucci-3	IA 20		ROR1KO	-1	IA 20	ROR1KO	-3	IA 20
H	Fucci-2			media			ROR1KO	-2		media		

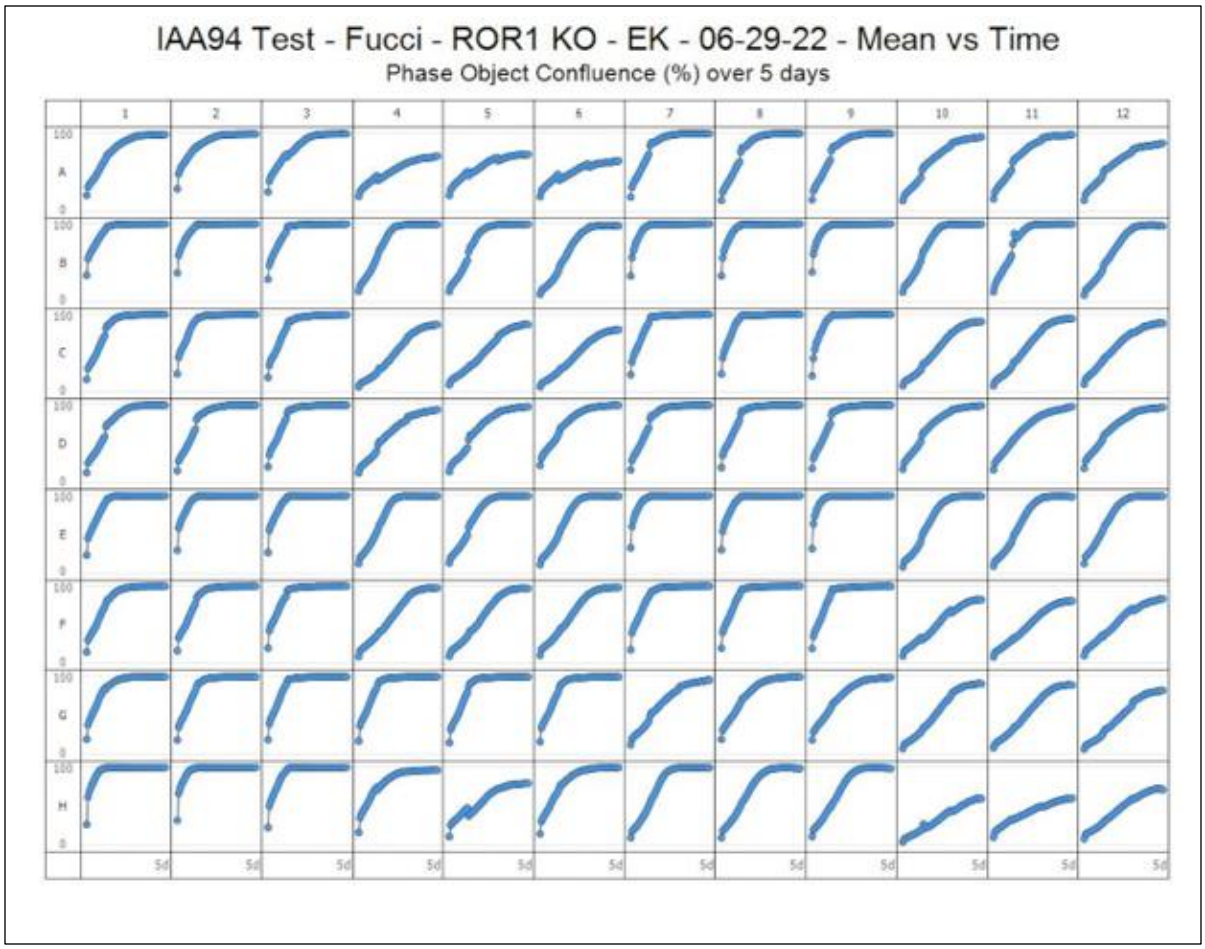

Figure 3.g: **96-well plate set up and percent confluence micrographs of PC3 Fucci clone 1, clone 2, and clone 4 treated with CLIC1 inhibitor, IAA94, in real time cell imaging analysis.** The top panel shows the 96-well plate set up for the treatment of PC3 Fucci and PC3 ROR1KO cells with IAA94. The bottom panel shows micrographs of the percent confluence as time advanced in all 96 wells.

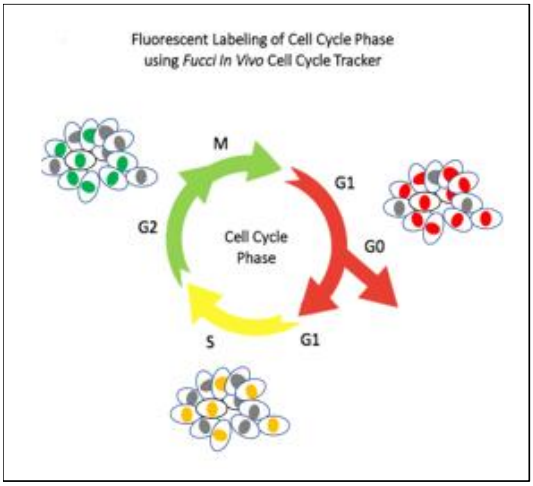

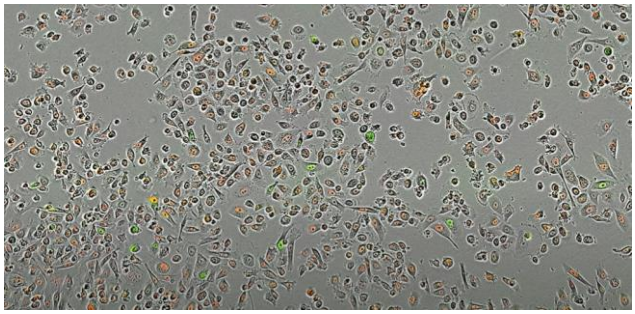

PC3 Fucci2BL image from scan taken in the Incucyte

Figure 4.a: **Fluorescent labeling of cell cycle phases using Fucci2BL live cell cycle tracker system.**

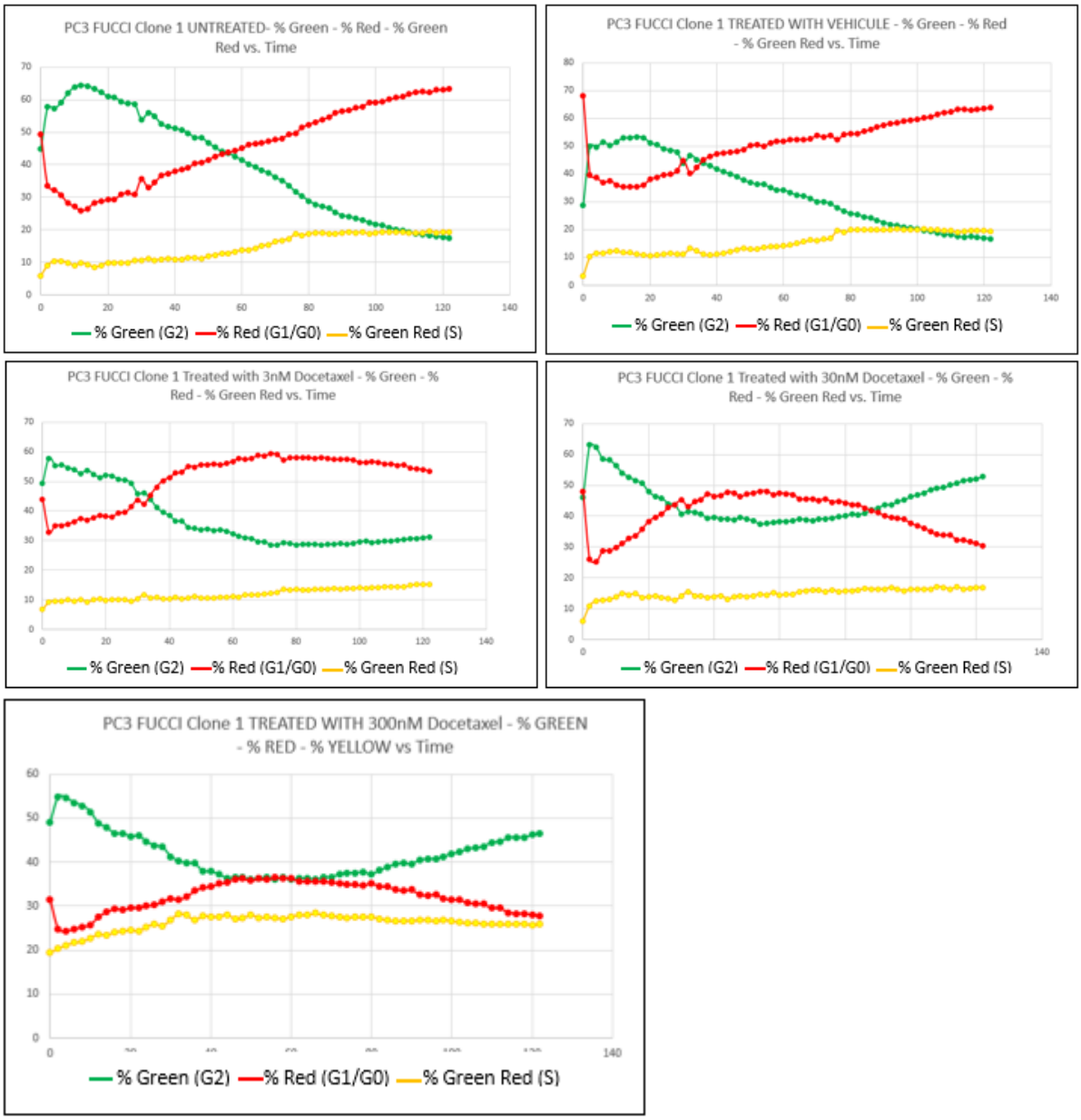

Figure 4.b: **Docetaxel impedes the cell cycle in PC3 Clone 1 cells expressing the Fucci live cell cycle tracking system resulting in inversion of final G1:G2 ratio.** The green (G2), red (G1 or G0), yellow (S, green + red) counts were measured through the software embedded in the IncuCyte. From these numbers, the percent green, red, and yellow count were calculated. The graphs show the percent green, red, and yellow count as time advanced. The images were taken every two hours.

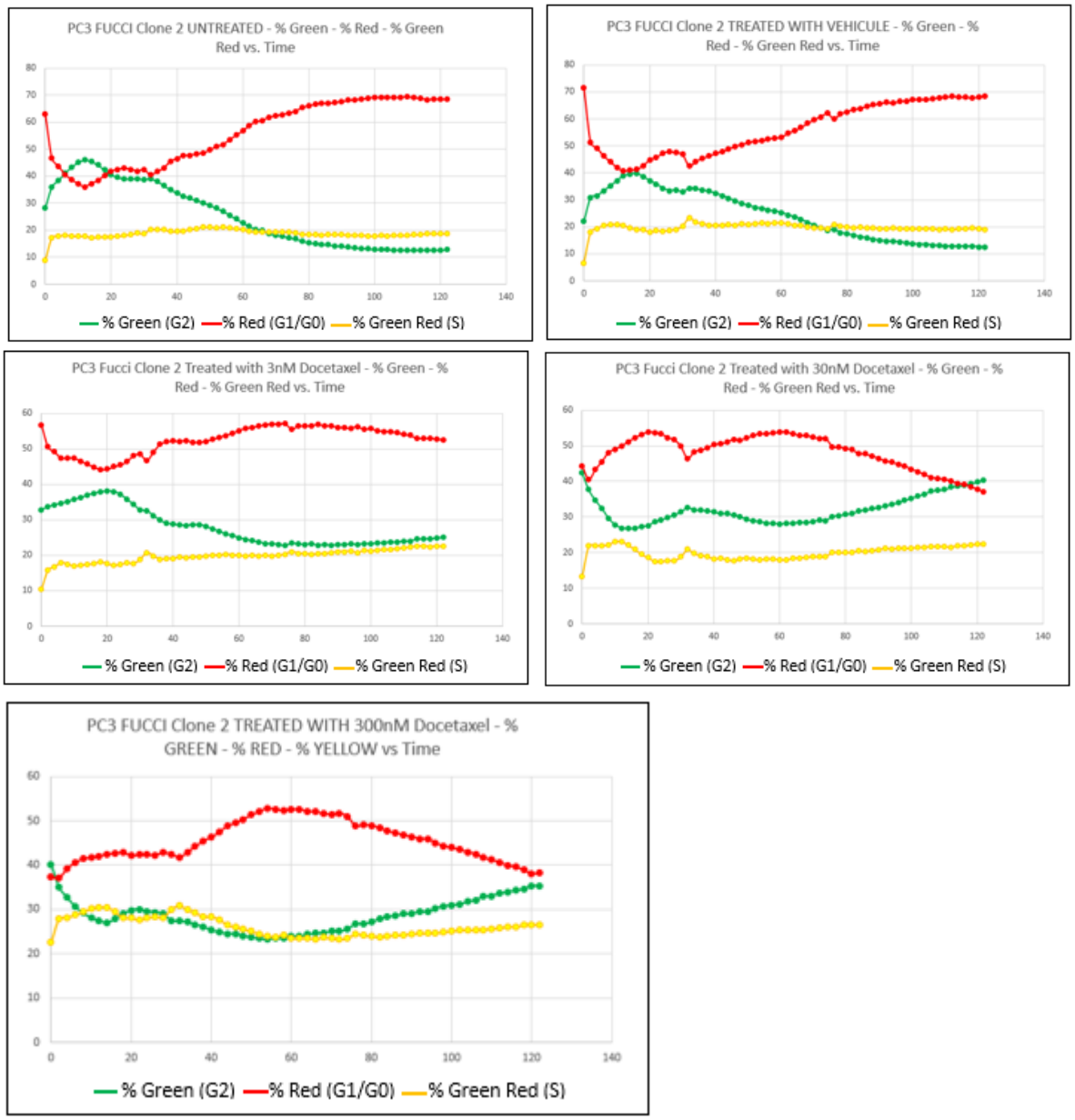

Figure 4.c: **Docetaxel impedes the cell cycle in PC3 Clone 2 cells expressing the Fucci live cell cycle tracking system resulting in inversion of final G1:G2 ratio.** The green (G2), red (G1 or G0), yellow (S, green + red) counts were measured through the software embedded in the IncuCyte. From these numbers, the percent green, red, and yellow count were calculated. The graphs show the percent green, red, and yellow count as time advanced. The images were taken every two hours.

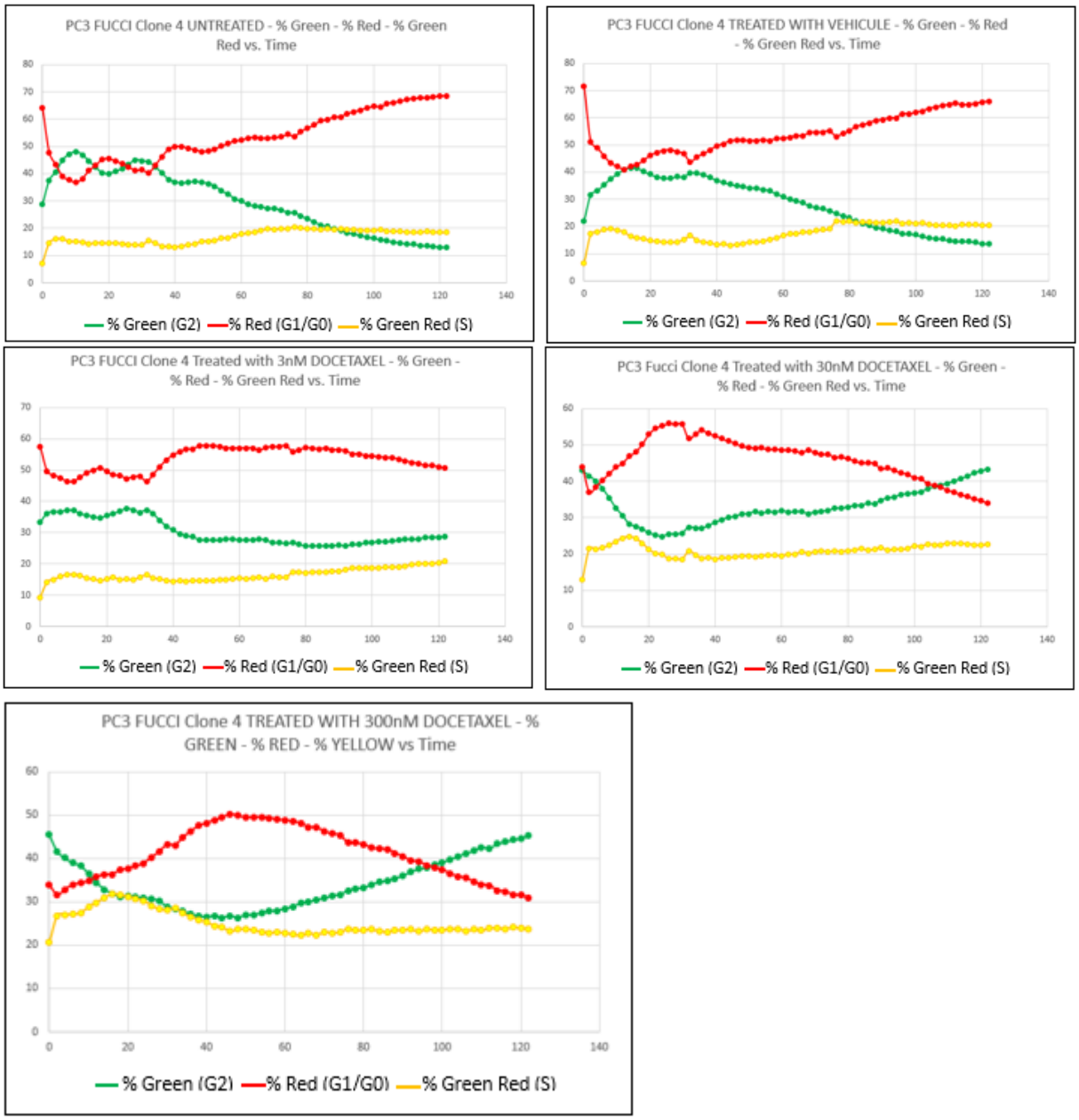

Figure 4.d: **Docetaxel impedes the cell cycle in PC3 Clone 4 cells expressing the Fucci live cell cycle tracking system resulting in inversion of final G1:G2 ratio.** The green (G2), red (G1 or G0), yellow (S, green + red) counts were measured through the software embedded in the IncuCyte. From these numbers, the percent green, red, and yellow count were calculated. The graphs show the percent green, red, and yellow count as time advanced. The images were taken every two hours.

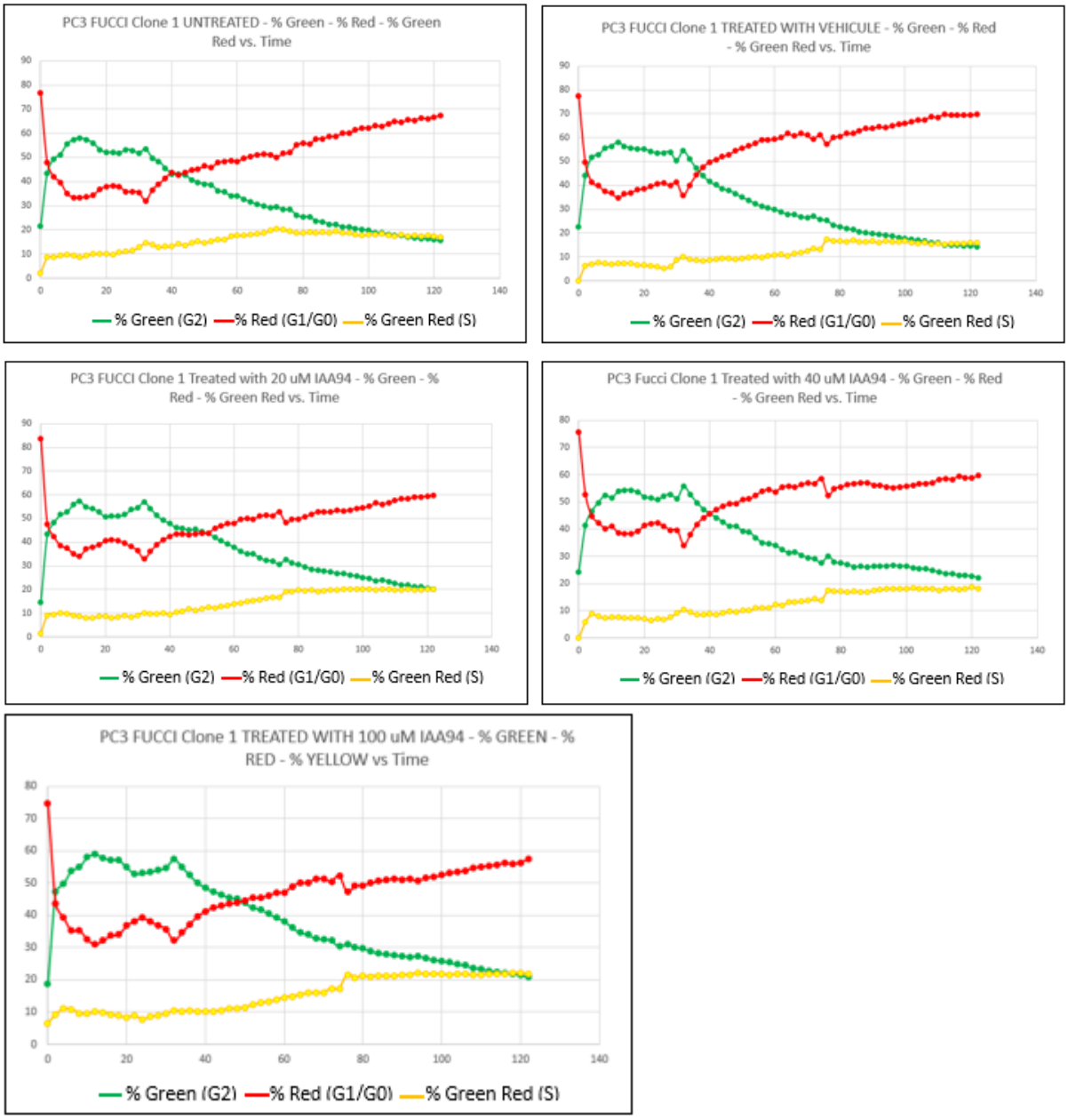

Figure 5.a: **Treatment with IAA94 and its effect on the cell cycle of PC3 Fucci Clone 1**

The green (G2), red (G1 or G0), yellow (S, green + red) counts were measured through the software embedded in the IncuCyte. From these numbers, the percent green, red, and yellow count were calculated. The graphs show the percent green, red, and yellow count as time advanced. The images were taken every two hours.

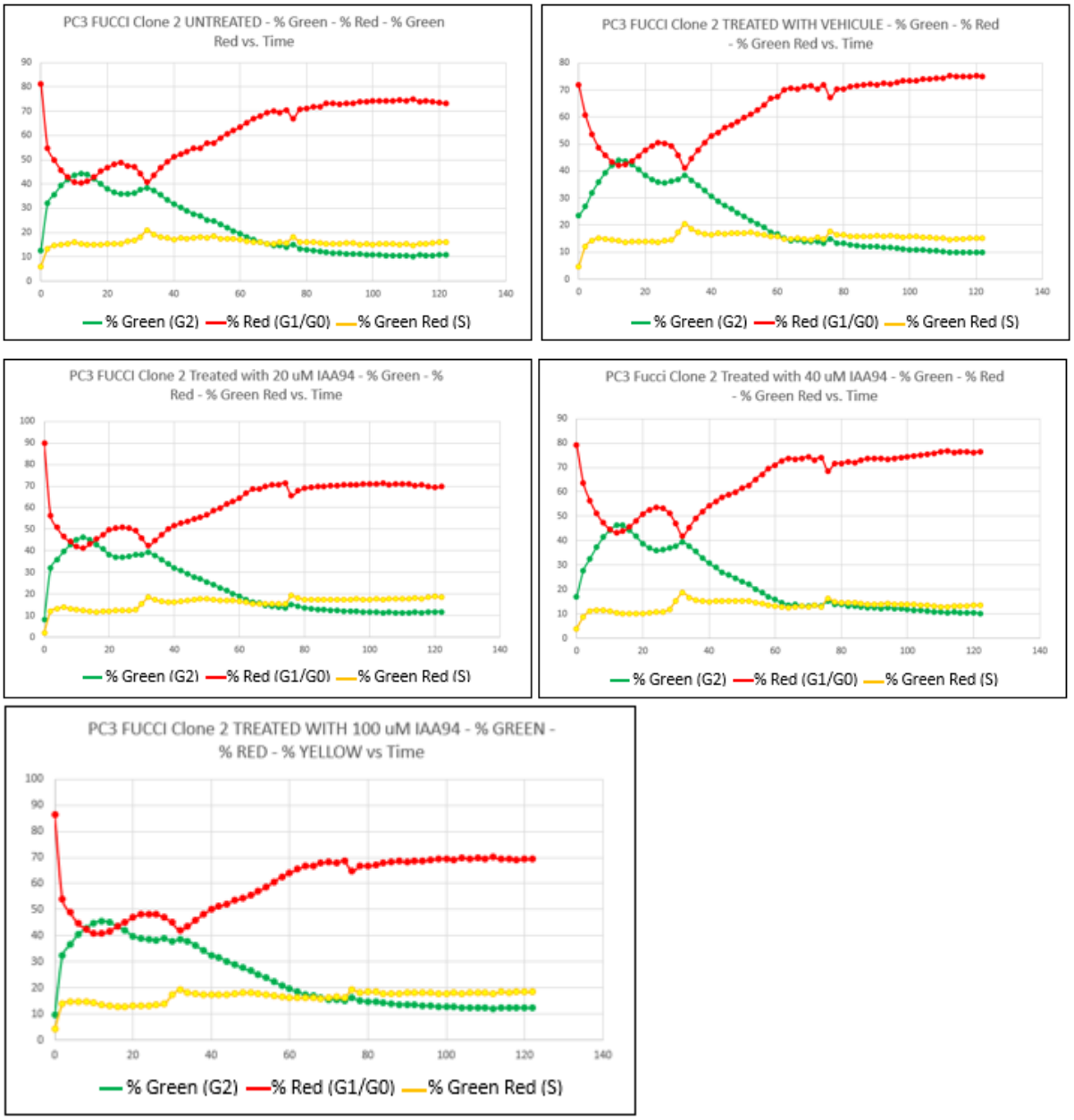

Figure 5.b: **Treatment with IAA94 and its effect on the cell cycle of PC3 Fucci Clone 2**

The green (G2), red (G1 or G0), yellow (S, green + red) counts were measured through the software embedded in the IncuCyte. From these numbers, the percent green, red, and yellow count were calculated. The graphs show the percent green, red, and yellow count as time advanced. The images were taken every two hours.

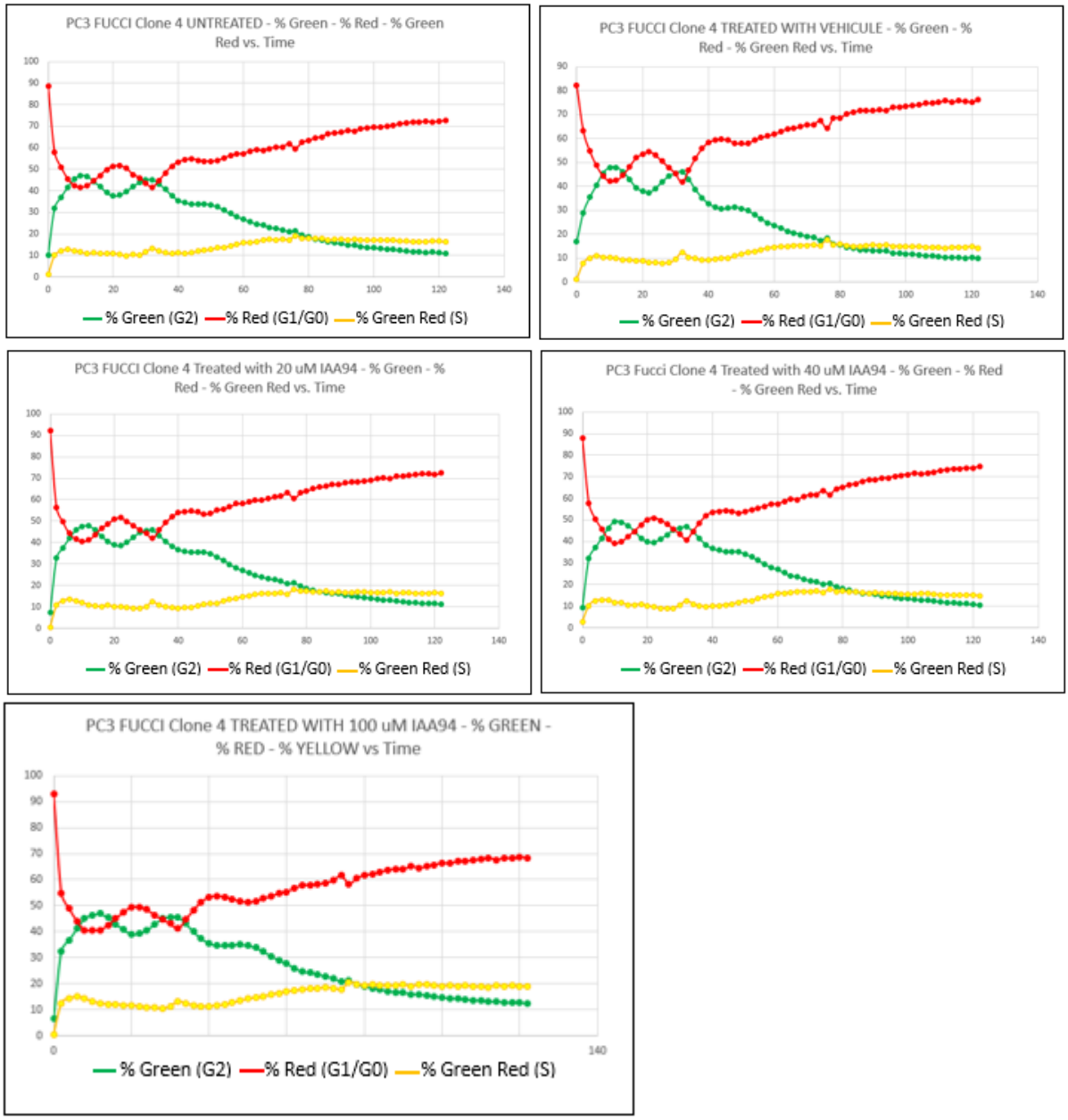

Figure 5.c: **Treatment with IAA94 and its effect on the cell cycle of PC3 Fucci Clone 4**

The green (G2), red (G1 or G0), yellow (S, green + red) counts were measured through the software embedded in the IncuCyte. From these numbers, the percent green, red, and yellow count were calculated. The graphs show the percent green, red, and yellow count as time advanced. The images were taken every two hours.

CHAPTER 3 DISCUSSION

Effect of Docetaxel

Facing the urgent need for finding therapies against prostate cancer, we propose two pathways, ROR1 and CLIC1 pathways, as potential targets that could work either alone or in synergy with standard of care chemotherapy drug Docetaxel. Based on our results, the treatment of the prostate cancer cell lines, PC3 Fucci clones, with Docetaxel was proven to be effective for inhibiting cell proliferation. The sensitivity of each clone to Docetaxel varied slightly. Upon treatment with 300nM and 30nM Docetaxel, PC3 Fucci clone 1 was the most sensitive to Docetaxel, followed by clone 4, and clone 2. Interestingly, before the assay was performed, we noticed that PC3 clone 2 was growing more rapidly than the other clones. This reveals to us that the rate at which the cells were growing before the assay might determine the extent of the results. Our results, thus, could be an important factor in explaining why different individuals have different reactions to the same treatment.

Overall, the data agrees with what we anticipated based on Docetaxel's features. In fact, the drug causes dysregulation in the dynamics of the microtubules, which is expected to prevent the cells from going through mitosis. We believe this is the reason why treatment of the cells with 300nM and 30nM Docetaxel led to a block in mitosis, which, we think, caused a growth plateau at low confluence levels. In fact, we noticed the coincidence between the timeline the cells reached a growth plateau and the timeline for the detection of higher percent green fluorescence, revealing that the drug led to cell cycle arrest in G2 phase.

Another question we were interested in was whether better outcomes in cancer cell inhibition could be achieved by combining Docetaxel treatment with inhibition of the ROR1 pathway. Our results from knocking out ROR1 in PC3 prostate cancer cells, followed by

Docetaxel treatment support this hypothesis. We found that by preventing ROR1 expression, Docetaxel treatment led to more cell proliferation inhibition. This suggests potential better outcomes in the clinic if a ROR1 chemical inhibitor can be found to include with Docetaxel treatment.

Effect of the CLIC1 inhibitor, IAA94

Treatment of PC3 Fucci and PC3 ROR1KO cells with IAA94 did not reveal any inhibitory effect on cell proliferation. In fact, based on the measurements with the IncuCyte, the cells treated with 20uM, 40uM, and 100uM IAA94 still reached high confluence levels. The effect of IAA94 on the cell cycle was not detected as well. Our original theory was that CLIC1 translocation to the cell membrane contributes to prostate cancer progression and metastasis. Therefore, we hypothesized that by treating the cells with IAA94, which is known to be a CLIC1 inhibitor, we would be able to inhibit the translocation of CLIC1 to the membrane. As a result, we would expect a decrease in cancer progression, which could be observed here by a decrease in cell proliferation and an arrest in the cell cycle. The fact that we did not observe our anticipated results may be caused by multiple factors. The stock solution of IAA94 was at a concentration of 400mM mixed in 100% ethanol. To perform the assay, we proceeded through a dilution series to obtain the desired concentrations of 20uM, 40uM, and 100uM IAA94 to treat the cells. During the dilution series, we noticed a white precipitate on the pipette tip and a white artifact in the solution as we were making the first dilution. Thus, we suspect that the drug went out of solution. If that is the case, it would mean that the cells were not tested with the intended concentrations of IAA94, but instead with traces of the drug. Therefore, we would not be able to see the effects of the drug because it was not present at the optimum concentration. A proposed solution might be to find strategies to properly mix the drug and cells' growth media.

Another explanation might be that the assays performed with IAA94 were not the most appropriate based on the features of the drug. In fact, CLIC1 translocation is known to be involved in cancer progression by promoting cell migration. Therefore, since IAA94 is intended to prevent CLIC1 translocation, a better assay to assess its effectiveness would be the scratch assay. It can be performed using the IncuCyte and is specifically designed to investigate cell migration. We performed preliminary data using the PC3 Fucci clones 2 and 4 without any drug treatments, but more optimizations need to be done. The overall idea will be to test the effect of IAA94 and other CLIC1 inhibitors on cell migration using the scratch assay. The other theory was that CLIC1 has already translocated to the membrane in our cell lines. We plan on verifying the position of CLIC1 using Immunohistochemistry staining. Overall, our results do not support that IAA94 has inhibitory effect on PC3 Fucci and PC3 ROR1KO cell proliferation obtained. This might be caused by one or a combination of the theories described above.

Conclusion

A real time Incucyte proliferation assay was optimized for our study and showed reproducible cell proliferation curves and live cell cycle tracking for the prostate cell lines PC3 Fucci and PC3 ROR1. Using a Fucci2BL cell cycle reporter, we found that increasing doses of docetaxel resulted in G2 arrest in PC3 cells. In addition, Docetaxel treatment resulted in inhibition of PC3 cell proliferation at lower doses when ROR1 was knocked out using CRISPR/Cas9. We anticipate that even lower concentrations of Docetaxel will show G2 arrest in PC3 ROR1 KO Fucci cells, than is needed for PC3 Fucci cells. Increasing doses of the CLIC1 inhibitor, IAA94, did not affect the proliferation or cell cycle of PC3 Fucci or PC3 ROR1 KO cells. Future studies will test the effect of newly synthesized IAA94-derived compounds in cell proliferation, cell cycle and on cell migration using the Incucyte Scratch assay.

Chapter 1, 2, and 3 includes work in preparation for submission for publication Jamillah Murtadha, **Evodie Koutouan**, Chris Oh, Michelle Muldong, Niloofar Etemadfard, Hae Soo Choo, Navyaa Sinha, Sanghee Lee, Christina Wu, Catriona Jamieson, Christopher Kane, Terry Gaasterland, Rana Mckay, Nicholas Cacalano, Anna Kulidjian, Charles Prussak, and Christina Jamieson.

The thesis author was the second author of this paper.

REFERENCES

Butler MT, Wallingford JB. Planar Cell Polarity in Development and Disease. *Nat Rev Mol Cell Biol* (2017) 18:375–88. 10.1038/nrm.2017.11

Bu, Y. & Diehl, J. A. PERK Integrates Oncogenic Signaling and Cell Survival During Cancer Development. J Cell Physiol 231, 2088- 2096, doi:10.1002/jcp.25336 (2016).

Chen, Y., Chen, L., Yu, J., Ghia, E. M., Choi, M. Y., Zhang, L., Zhang, S., Sanchez-Lopez, E., Widhopf, G. F., 2nd, Messer, K., Rassenti, L. Z., Jamieson, C., & Kipps, T. J. Cirmtuzumab blocks Wnt5a/ROR1 stimulation of NF-kappaB to repress autocrine STAT3 activation in chronic lymphocytic leukemia. Blood. 2019 ;134(13) :1084-94.

Cianci F, Verduci I. Transmembrane Chloride Intracellular Channel 1 (tmCLIC1) as a Potential Biomarker for Personalized Medicine. J Pers Med. 2021 Jul 5;11(7):635. doi: 10.3390/jpm11070635. PMID: 34357102; PMCID: PMC8307889.

Crona, D. J. & Whang, Y. E. Androgen Receptor-Dependent and -Independent Mechanisms Involved in Prostate Cancer Therapy Resistance. Cancers (Basel) 9, doi:10.3390/cancers9060067 (2017).

Cui, B., Ghia, E. M., Chen, L., Rassenti, L. Z., DeBoever, C., Widhopf, G. F., 2nd, Yu, J., Neuberg, D. S., Wierda, W. G., Rai, K. R., Kay, N. E., Brown, J. R., Jones, J. A., Gribben, J. G., Frazer, K. A., & Kipps, T. J. High-level ROR1 associates with accelerated disease progression in chronic lymphocytic leukemia. Blood. 2016 ;128(25) :2931-40.

De A. Wnt/Ca2+ Signaling Pathway: A Brief Overview. *Acta Biochim Biophys Sin (Shanghai)* (2011) 43:745–56. 10.1093/abbs/gmr079

deSolms, S. J., Woltersdorf, O. W., Jr., Cragoe, E. J., Jr., Watson, L. S. & Fanelli, G. M., Jr. (Acylaryloxy)acetic acid diuretics. 2. (2- Alkyl-2-aryl-1-oxo-5-indanyloxy) acetic acids. J Med Chem 21, 437-443, doi:10.1021/jm00203a006 (1978).

Dhingra R., Sharma T., Singh S., Sharma S., Tomar P., Malhotra M., Bhardwaj T.R. Enzalutamide: A novel anti-androgen with prolonged survival rate in CRPC patients. *Mini Rev. Med. Chem.* 2013; 13:1475–1486. doi: 10.2174/13895575113139990003.

Fizazi, K., Scher, H. I., Molina, A., Logothetis, C. J., Chi, K. N., Jones, R. J., Staffurth, J. N., North, S., Vogelzang, N. J., Saad, F., Mainwaring, P., Harland, S., Goodman, O. B., Jr, Sternberg, C. N., Li, J. H., Kheoh, T., Haqq, C. M., de Bono, J. S., & COU-AA-301 Investigators Abiraterone acetate for treatment of metastatic castration-resistant prostate cancer: Final overall survival analysis of the COU-AA-301 randomised, double-blind, placebo-controlled phase 3 study. *Lancet Oncol.* 2012; 13:983–992. doi: 10.1016/S1470-2045(12)70379-0.

Gillessen, S., Attard, G., Beer, T. M., Beltran, H., Bjartell, A., Bossi, A., Briganti, A., Bristow, R. G., Chi, K. N., Clarke, N., Davis, I. D., de Bono, J., Drake, C. G., Duran, I., Eeles, R., Efstathiou, E., Evans, C. P., Fanti, S., Feng, F. Y., Fizazi, K., … Omlin, A. Management of Patients with

Advanced Prostate Cancer: Report of the Advanced Prostate Cancer Consensus Conference 2019. Eur Urol 77, 508-547, doi: 10.1016/j.eururo.2020.01.012 (2020).

Grasso, C. S., Wu, Y. M., Robinson, D. R., Cao, X., Dhanasekaran, S. M., Khan, A. P., Quist, M. J., Jing, X., Lonigro, R. J., Brenner, J. C., Asangani, I. A., Ateeq, B., Chun, S. Y., Siddiqui, J., Sam, L., Anstett, M., Mehra, R., Prensner, J. R., Palanisamy, N., Ryslik, G. A., Vandin, F., Raphael B. J., Kunju, L. P., Rhodes, D. R., Pienta, K.J., Chinnaivan, A. M., Tomlins, S. A. The mutational landscape of lethal castration-resistant prostate cancer. *Nature.* 2012; 487:239–243. doi: 10.1038/nature11125.

Gururaja Rao, S., Patel, N. J. & Singh, H. Intracellular Chloride Channels: Novel Biomarkers in Diseases. Front Physiol 11, 96, doi:10.3389/fphys.2020.00096 (2020).

Huang, L., Pu, Y., Hu, W. Y., Birch, L., Luccio-Camelo, D., Yamaguchi, T., & Prins, G. S. The role of Wnt5a in prostate gland development. Dev Biol. 2009;328(2):188-99.

Jordan MA. Mechanism of action of antitumor drugs that interact with microtubules and tubulin. Curr Med Chem Anticancer Agents. 2002 Jan;2(1):1-17. doi: 10.2174/1568011023354290. PMID: 12678749.

Jordan MA, Wilson L. Microtubules as a target for anticancer drugs. Nat Rev Cancer. 2004 Apr;4(4):253-65. doi: 10.1038/nrc1317. PMID: 15057285.

Kirby M., Hirst C., Crawford E.D. Characterising the castration-resistant prostate cancer population: A systematic review. *Int. J. Clin. Pract.* 2011; 65:1180–1192. doi: 10.1111/j.1742-1241.2011.02799. x.

Landry, D. W., Reitman, M., Cragoe, E. J., Jr. & Al-Awqati, Q. Epithelial chloride channel. Development of inhibitory ligands. J Gen Physiol 90, 779-798, doi:10.1085/jgp.90.6.779 (1987).

Lathrop, A. E. & Loeb, L. Further investigations on the origin of tumors in mice. III. On the part played by internal secretion in the spontaneous development of tumors. J Cancer Res 1, 1-19 (1916).

Lee, J. S., Leem, S. H., Lee, S. Y., Kim, S. C., Park, E. S., Kim, S. B., Kim, S. K., Kim, Y. J., Kim, W. J., & Chu, I. S. Expression signature of E2F1 and its associated genes predict superficial to invasive progression of bladder tumors. J Clin Oncol 28, 2660-2667, doi:10.1200/JCO.2009.25.0977 (2010).

Lee, G. T., Kwon, S. J., Kim, J., Kwon, Y. S., Lee, N., Hong, J. H., Jamieson, C., Kim, W. J., & Kim, I. Y. WNT5A induces castration-resistant prostate cancer via CCL2 and tumour-infiltrating macrophages. Br J Cancer. 2018;118(5):670-8.

Li, B. P., Mao, Y. T., Wang, Z., Chen, Y. Y., Wang, Y., Zhai, C. Y., Shi, B., Liu, S. Y., Liu, J. L., & Chen, J. Q. CLIC1 Promotes the Progression of Gastric Cancer by Regulating the MAPK/AKT Pathways. Cell Physiol Biochem 46, 907-924, doi:10.1159/000488822 (2018).

Lin, G., Huang, T., Zhang, X., & Wang, G. Deubiquitinase USP35 stabilizes BRPF1 to activate mevalonate (MVA) metabolism during prostate tumorigenesis. *Cell Death Discov.* **8**, 453 (2022). https://doi.org/10.1038/s41420-022-01231-x

Luo, J., Wang, D., Wan, X., Xu, Y., Lu, Y., Kong, Z., Li, D., Gu, W., Wang, C., Li, Y., Ji, C., Gu, S., & Xu, Y. Crosstalk Between AR and Wnt Signaling Promotes Castration-Resistant Prostate Cancer Growth. Onco Targets Ther. 2020; 13:9257-67.

Ma, P. F., Chen, J. Q., Wang, Z., Liu, J. L. & Li, B. P. Function of chloride intracellular channel 1 in gastric cancer cells. World J Gastroenterol 18, 3070-3080, doi:10.3748/wjg. v18.i24.3070 (2012).

Peretti, M., Raciti, F. M., Carlini, V., Verduci, I., Sertic, S., Barozzi, S., Garré, M., Pattarozzi, A., Daga, A., Barbieri, F., Costa, A., Florio, T., & Mazzanti, M. Mutual Influence of ROS, pH, and CLIC1 Membrane Protein in the Regulation of G1-S Phase Progression in Human Glioblastoma Stem Cells. Mol Cancer Ther 17, 2451-2461, doi: 10.1158/1535-7163.MCT-17-1223 (2018).

Perez EA. Microtubule inhibitors: Differentiating tubulin-inhibiting agents based on mechanisms of action, clinical activity, and resistance. Mol Cancer Ther. 2009 Aug;8(8):2086-95. doi: 10.1158/1535-7163.MCT-09-0366. Epub 2009 Aug 11. Erratum in: Mol Cancer Ther. 2012 Jun;11(6):1381. PMID: 19671735.

Pineda, G., Lennon, K. M., Delos Santos, N. P., Lambert-Fliszar, F., Riso, G. L., Lazzari, E., Marra, M. A., Morris, S., Sakaue-Sawano, A., Miyawaki, A., & Jamieson, C. H. M. (2016). Tracking of Normal and Malignant Progenitor Cell Cycle Transit in a Defined Niche. Scientific Reports, 6(1), 23885. https://doi.org/10.1038/srep23885

Sandsmark, E., Hansen, A. F., Selnæs, K. M., Bertilsson, H., Bofin, A. M., Wright, A. J., Viset, T., Richardsen, E., Drabløs, F., Bathen, T. F., Tessem, M. B., & Rye, M. B. A novel non-canonical Wnt signature for prostate cancer aggressiveness. Oncotarget. 2017;8(6):9572-86.

Setti, M., Savalli, N., Osti, D., Richichi, C., Angelini, M., Brescia, P., Fornasari, L., Carro, M. S., Mazzanti, M., & Pelicci, G. Functional role of CLIC1 ion channel in glioblastoma-derived stem/progenitor cells. J Natl Cancer Inst 105, 1644- 1655, doi:10.1093/jnci/djt278 (2013).

Singh, H. Two decades with dimorphic Chloride Intracellular Channels (CLICs). FEBS Lett 584, 2112-2121, doi: 10.1016/j.febslet.2010.03.013 (2010).

Surveillance, Epidemiology, and End Results (SEER) Program, Preliminary Cancer Incidence Rate Estimates for 2017, and diagnosis years 2000 to 2017, SEER 18, National Cancer Institute. Bethesda, MD, https://seer.cancer.gov/statistics/preliminary-estimates/, based on the February 2019 SEER data submission and the November 2018 SEER data submission. Posted to the SEER web site, September 2019. SEER. Retrieved June 14, 2022, from https://seer.cancer.gov/statfacts/html/prost.html

Tian, Y., Guan, Y., Jia, Y., Meng, Q. & Yang, J. Chloride intracellular channel 1 regulates prostate cancer cell proliferation and migration through the MAPK/ERK pathway. Cancer Biother Radiopharm 29, 339-344, doi:10.1089/cbr.2014.1666 (2014).

Ulmasov, B., Bruno, J., Woost, P. G. & Edwards, J. C. Tissue and subcellular distribution of CLIC1. BMC Cell Biol 8, 8, doi:10.1186/1471-2121-8-8 (2007).

Ummanni, R., Junker, H., Zimmermann, U., Venz, S., Teller, S., Giebel, J., Scharf, C., Woenckhaus, C., Dombrowski, F., & Walther, R. Prohibitin identified by proteomic analysis of prostate biopsies distinguishes hyperplasia and cancer. Cancer Lett 266, 171-185, doi : 10.1016/j.canlet.2008.02.047 (2008).

Valenzuela, S. M., Martin, D. K., Por, S. B., Robbins, J. M., Warton, K., Bootcov, M. R., Schofield, P. R., Campbell, T. J., & Breit, S. N. Molecular cloning and expression of a chloride ion channel of cell nuclei. J Biol Chem 272, 12575-12582, doi:10.1074/jbc.272.19.12575 (1997).

Vlachostergios, P. J., Puca, L. & Beltran, H. Emerging Variants of Castration-Resistant Prostate Cancer. Curr Oncol Rep 19, 32, doi:10.1007/s11912-017-0593-6 (2017).

Wang, P., Zeng, Y., Liu, T., Zhang, C., Yu, P. W., Hao, Y. X., Luo, H. X., & Liu, G. Chloride intracellular channel 1 regulates colon cancer cell migration and invasion through ROS/ERK pathway. World J Gastroenterol 20, 2071-2078, doi:10.3748/wjg. v20.i8.2071 (2014).

Wang, P., Zhang, C., Yu, P., Tang, B., Liu, T., Cui, H., & Xu, J. Regulation of colon cancer cell migration and invasion by CLIC1-mediated RVD. Mol Cell Biochem 365, 313-321, doi:10.1007/s11010-012-1271-5 (2012).

Woltersdorf, O. W., Jr., deSolms, S. J., Schultz, E. M. & Cragoe, E. J., Jr. (Acylaryloxy)acetic acid diuretics. 1. (2-Alkyl- and 2,2- dialkyl-1-oxo-5-indanyloxy) acetic acids. J Med Chem 20, 1400-1408, doi:10.1021/jm00221a010 (1977).

Xu, Y., Zhu, J., Hu, X., Wang, C., Lu, D., Gong, C., Yang, J., & Zong, L. CLIC1 Inhibition Attenuates Vascular Inflammation, Oxidative Stress, and Endothelial Injury. PLoS One 11, e0166790, doi: 10.1371/journal.pone.0166790 (2016).

Yamamoto, H., Oue, N., Sato, A., Hasegawa, Y., Yamamoto, H., Matsubara, A., Yasui, W., & Kikuchi, A. Wnt5a signaling is involved in the aggressiveness of prostate cancer and expression of metalloproteinase. Oncogene. 2010;29(14):2036-46.

Yu, J., Chen, L., Cui, B., Widhopf, G. F., 2nd, Shen, Z., Wu, R., Zhang, L., Zhang, S., Briggs, S. P., & Kipps, T. J. Wnt5a induces ROR1/ROR2 heterooligomerization to enhance leukemia chemotaxis and proliferation. J Clin Invest. 2016 ;126(2) :585-98.

Yu, J., Chen, L., Cui, B., Wu, C., Choi, M. Y., Chen, Y., Zhang, L., Rassenti, L. Z., Widhopf Ii, G. F., & Kipps, T. J. Cirmtuzumab inhibits Wnt5a-induced Rac1 activation in chronic lymphocytic leukemia treated with ibrutinib. Leukemia. 2017;31(6):1333-9.

Zhang, S., Zhang, H., Ghia, E. M., Huang, J., Wu, L., Zhang, J., Lam, S., Lei, Y., He, J., Cui, B., Widhopf, G. F., 2nd, Yu, J., Schwab, R., Messer, K., Jiang, W., Parker, B. A., Carson, D. A., & Kipps, T. J. Inhibition of chemotherapy resistant breast cancer stem cells by a ROR1 specific antibody. Proc Natl Acad Sci U S A. 2019;116(4):1370-7.

Zhang, S., Chen, L., Cui, B., Chuang, H. Y., Yu, J., Wang-Rodriguez, J., Tang, L., Chen, G., Basak, G. W., & Kipps, T. J. ROR1 is expressed in human breast cancer and associated with enhanced tumor-cell growth. PLoS One. 2012;7(3): e31127.

Zhang, S., Chen, L., Wang-Rodriguez, J., Zhang, L., Cui, B., Frankel, W., Wu, R., & Kipps, T. J. The onco-embryonic antigen ROR1 is expressed by a variety of human cancers. Am J Pathol. 2012;181(6):1903-10.

Zhao Y, Zhang D, Guo Y, Lu B, Zhao ZJ, Xu X, Chen Y. Tyrosine Kinase ROR1 as a Target for Anti-Cancer Therapies. Front Oncol. 2021 May 28; 11:680834. doi: 10.3389/fonc.2021.680834. PMID: 34123850; PMCID: PMC8193947.

Zhao, W., Lu, M. & Zhang, Q. Chloride intracellular channel 1 regulates migration and invasion in gastric cancer by triggering the ROS-mediated p38 MAPK signaling pathway. Mol Med Rep 12, 8041-8047, doi:10.3892/mmr.2015.4459 (2015).